Generalized Scaling Hypothesis in Multicomponent Systems. I. Classification of Critical Points by Order and Scaling at Tricritical Points*

T. S. Chang,† Alex Hankey,‡ and H. Eugene Stanley§
Department of Physics, Massachusetts Institute of Technology, Cambridge, Massachusetts 02139
(Received 10 October 1972; revised manuscript received 29 January 1973)

The goal of this work is to provide an analysis of spaces of critical points for multicomponent systems. First, we propose the geometric concept of order $\mathcal{O}$ for critical points; we distinguish it from a previous definition of a "multicritical" point. Specifically, we may define the intersection of spaces of critical points of order $\mathcal{O}$ to be a space of critical points of order $(\mathcal{O}+1)$. Ordinary critical points are defined to be of order $\mathcal{O}=2$, so that the tricritical points introduced by Griffiths are of order $\mathcal{O}=3$. We discuss more general examples of critical spaces of order $\mathcal{O}=3$ which are known for a wide variety of systems; we also propose several examples of models of magnetic systems showing critical points of order $\mathcal{O}=4$—i.e., systems having *intersecting lines of tricritical points.* The analysis of critical and coexistence spaces also provides a new form of the Gibbs phase rule suitable for complex magnetic models. Next we define—for the critical points of order $\mathcal{O}$ of which examples have been given—special directions in terms of which to make a scaling hypothesis. We give the hypothesis for simple systems and then for tricritical points, and then, in a subsequent paper, part II, the special directions are used to make a scaling hypothesis at spaces of critical points of any order. Certain predictions (e.g., scaling laws and "single-power" scaling functions) follow in a simple and straightforward fashion. We consider the scaling hypothesis at a critical space of order $\mathcal{O}$ in terms of a group of transformations. We can define a set of invariants of the group. It is possible, for $\mathcal{O}\geq 3$, to make a *second* scaling hypothesis for the space of order $\mathcal{O}-1$ using certain of these invariants as *independent* variables. This is advantageous because certain "double-power" scaling functions then follow directly; these predict that for $\mathcal{O}=3$, experimental data collapse from a *volume* onto a *line*. This prediction is to be contrasted with ordinary scaling functions, which predict that data collapse by only a single dimension (e.g., from a volume onto a surface or from a surface onto a line).

I. INTRODUCTION: THE ORDER OF A CRITICAL POINT

The purpose of this work is (i) to propose the concept of the "order" of a critical point, (ii) to give examples of critical points of orders three and four, and (iii) to present a form of the scaling hypothesis for spaces of *arbitrary* order. The work is divided into two parts. In this paper (I), we focus upon concrete examples illustrating critical points and scaling at critical points of order three, while in a subsequent paper[1] (II), we consider scaling for spaces of arbitrary order. Firstly, we must develop the concept of the order of a critical point, and that is the task of this section.

The scaling hypothesis was originally formulated for the critical point of a simple magnet and a simple fluid.[2-4] These systems each have two purely intensive variables [(H, T) and (P, T), respectively]. Such variables we call *fields*, adopting the terminology of Griffiths and Wheeler.[5]

A very wide variety of physical systems whose critical phenomena are under active study have more than two field variables; two common examples are antiferromagnets and binary mixtures. In such systems, one can have lines (or, in general, spaces of dimension larger than one) of critical points. Recently, special attention has come to focus on those systems for which *three* lines of critical points intersect, and the point of intersection has been called a *tricritical point* by Griffiths.[6]

The scaling hypothesis has recently been extended[7] to treat some (but not all) aspects of this novel type of "critical point". In this work we present a comprehensive scaling treatment of general multicomponent systems. First we give a detailed treatment of tricritical points. Our approach is then generalized to more complex situations.

One example of a more complex situation is a system for which *four* lines of critical points intersect; in a natural extension of Griffiths's terminology, Nagle and Bonner[8] have called such points tetracritical points. We show here that, in the particular case studied by those authors, *the tetracritical point is qualitatively the same as a tricritical point* in the sense that the formulation of the scaling hypothesis there is the same as at tricritical points.

Qualitatively different points ("spaces")[9] can be achieved in systems with more than three field variables; a more general scaling hypothesis is needed and correspondingly more predictions are obtained. These are discussed in detail in Paper II.

Two simple examples of systems with more than three field variables are provided by He^3-He^4 and ammonium chloride, and both these systems

show *lines* of tricritical points.

Liquid He^3-He^4 mixtures have thermodynamic variables $[P, T, \mu_4 - \mu_3, \eta]$, where P denotes pressure, T denotes temperature, μ_4 and μ_3 are the chemical potentials of He^4 and He^3, respectively, and η is a variable conjugate to the superfluid density. The "λ line" in the P-T plane becomes a two-dimensional surface of singularities with increasing mole fraction of He^3. This surface terminates at a line of special points,[10(a)] which is in fact a line of tricritical points.

Ammonium chloride possesses an order-disorder transition for which the transition temperature increases with increasing pressure, and changes from first order to second order at a tricritical point. If one replaces some of the hydrogen by deuterium in the ammonium group,[10(b)] then the position of the tricritical point (and the whole line of order-disorder transitions) changes. The variables are thus $(P, T, \mu_H - \mu_D, \eta)$, where η is a variable conjugate to the order parameter.

In a system of sufficient complexity, several lines of tricritical points can occur. A point of intersection of lines of tricritical points is qualitatively different from a point where lines of ordinary critical points intersect. This should be clear from the topology of the situation: At a line of tricritical points, surfaces of critical points meet, while at a point where lines of tricritical points intersect, several surfaces of critical points (bounded on each side by the tricritical lines) converge on the point.

To distinguish such points—and in general spaces of such points—we will refer to them as critical points of higher order, and we will associate a number with each order as follows. We define ordinary critical points to be of order $\mathfrak{o} = 2$; then a critical point (or space of points) of order $\mathfrak{o} + 1$ ($\mathfrak{o} \geq 2$) is defined to be a special point where lines (or spaces) of points of order $\mathfrak{o}$ intersect. Thus a tricritical point is of order $\mathfrak{o} = 3$ and a point of intersection of lines of tricritical points is of order $\mathfrak{o} = 4$.

Griffiths and Wheeler[5] reasoned that the dimensionality of a space of ordinary critical points (of order $\mathfrak{o} = 2$) is $(n - 2)$. In the systems we consider below the dimensionality, d, of a space of critical points of order $\mathfrak{o}$ is always one less than the dimensionality of the spaces of critical points of order $(\mathfrak{o} - 1)$ which intersect at it. Therefore, we find the value of d for arbitrary $\mathfrak{o}$ by induction from $\mathfrak{o} = 2$ to be, in these cases,

$$d = n - \mathfrak{o}, \tag{1.1}$$

where n is the total number of field (and fieldlike)[11] variables available.

Critical points of complex thermodynamic systems can also be analyzed by making the scaling hypothesis from the outset. The significant quantity is then the number of relevant scaling variables. Using the renormalization group, it has been suggested[12] how more than two relevant scaling variables can occur, but the geometry of the phase diagram was not considered at all. In most of the examples known to the authors, the number of significant scaling directions is equal to the order. This may not always be true for more complex systems [e.g., fluid mixtures, for which Eq. (1.1) may need modification, becoming $d \leq n - \mathfrak{o}$].

A specific example which demonstrates the importance of distinguishing the order of a critical point from the number of critical lines meeting there is the tetracritical point. This is a point of order $\mathfrak{o} = 3$ with true field variables (H, H_2, T), where H and H_2 are direct and staggered (i.e., wavelength 2 lattice sites) magnetic fields. When a fieldlike variable $\tilde{\mathfrak{R}}$ (the ratio of short- to long-range-interaction strengths) is also included, (i.e., $n = 4$), Eq. (1.1) indicates that the system has a line of critical points of order $\mathfrak{o} = 3$. This is verified in the analysis of Sec. III, where it is shown that in this model there are three surfaces of critical points of order $\mathfrak{o} = 2$, meeting at the line of points of order $\mathfrak{o} = 3$. The tetracritical point is simply a point on a smooth line of tricritical points; the "tetracritical point" arises because we have chosen a section of the four-dimensional $(H, H_2, T, \tilde{\mathfrak{R}})$ space that is tangent to the line of tricritical points, rather than a section which intersects it.

First we give, in Sec. II, examples of systems exhibiting spaces of critical points of order $\mathfrak{o} \geq 3$, and explain a convenient notation for the phase diagrams of such systems. This leads to an equation equivalent to the Gibbs phase rule.

In Sec. III we explicitly demonstrate the importance of distinguishing between the order of a critical point and the number of lines meeting at a critical point—the former leads to an essential increase in complexity, while the latter does not. To do this, we compare several one-dimensional Ising models with long-range interactions, all of which are exactly soluble.

Special directions at spaces of order $\mathfrak{o}$ are defined in Sec. IV; these are analogous to the strong and weak directions defined by Griffiths and Wheeler.[5] A way of deriving these directions for tricritical points using the renormalization group approach has been pointed out by Riedel and Wegner.[12(c)]

To make the formulation of a scaling hypothesis easier to follow, we give an account in Sec. V of the scaling hypothesis using generalized homogeneous functions and equations invariant under a one-parameter continuous group of transformations at points of order 2.

In Sec. VI we give a full account of the scaling

hypothesis at tricritical points and we include an account of a space of invariant variables as a very useful way to derive "double-power" scaling functions and to plot "crossover surfaces". These predictions have not yet been tested experimentally.

We present the scaling hypothesis at a critical point of arbitrary order in Paper II. The hypothesis is framed as a sequence of operations to be repeated as the hypothesis is formed successively at critical points of decreasing order. The proposed sequence is illustrated by detailed consideration of a system of Ising planes with a variable interplanar interaction.

II. SYSTEMS EXHIBITING CRITICAL POINTS OF ORDER HIGHER THAN TWO: NOTATION FOR SUCH POINTS

Critical points more complex than ordinary $\mathfrak{O}=2$ critical points have been found in many experimental and theoretical systems. Without doubt, the systems exhibiting the richest possibilities are multicomponent fluid mixtures; however, specific examples of critical points of order three or more in these systems have yet to be found.

Systems on which experiments have been analyzed are liquid helium,[10(a)] ammonium chloride,[10(b)] metamagnets,[13] and anisotropic antiferromagnets.[14] In addition, one-dimensional magnetic models provide a rich opportunity for theoretical and numerical investigations. Liquid helium[10(a)] and NH_4Cl[10(b)] provide excellent examples where there exist lines of tricritical points—as discussed in Sec. I. In metamagnets,[13] lines of tricritical points can be generated by introducing transverse fields, and also by introducing a parameter into the Hamiltonian which changes the strength of the interaction. Decreasing the latter causes the tricritical points to converge to a point on the temperature axis; this point is a critical point of order 4 and is treated in more detail below.

An anisotropic antiferromagnet,[14] which exhibits a spin-flop transition, contains a point in its phase diagram where two lines of ordinary critical points intersect a line of first-order transitions. This special point has an order of at least 3, but whether it is 3 or more has yet to be determined.

To be able to discuss phenomena in phase diagrams of any complexity easily, we introduce a notation for spaces of points where several phases coexist and for critical points of arbitrary order $\mathfrak{O}$. Critical spaces are denoted by an abbreviation of the notation CRS of Griffiths and Wheeler[5]; the order of the space will be given a preceding superscript and the dimensionality a subscript, and hence a critical space of order $\mathfrak{O}$ and dimensionality d is written as ${}^{\mathfrak{O}}R_d$. The relation between $\mathfrak{O}$, d, and the total number n of field (or fieldlike) variables, in general, is given by Eq. (1.1), $\mathfrak{O}=n-d$.

Coexistence spaces are designated by an abbreviation of the Griffiths-Wheeler notation CXS but now the number of coexisting phases is given by the preceding superscript; hence the general space of dimension d where p phases coexist is written as ${}^pX_d$. The equation analogous to Eq. (1.1) is

$$p=n-d+1. \tag{2.1}$$

The dimension d of the CXS may be interpreted as the number of "degrees of freedom", f, and for a chemical system n is one greater than the number of components c. Thus (2.1) is similar to the usual statement of the Gibbs phase rule, $p \geq c-f+2$, but it is in a form valid for all the systems considered in this work. The Gibbs phase rule contains an inequality because it refers to any phase diagram, even those in a restricted space of fields. For example, the ${}^2X_2$ in the H-T plane of a simple nearest-neighbor antiferromagnet (with field variables H, H_2, and T) satisfies Eq. (2.1) as an equality providing all three fields are considered, but as an inequality if only T and H are considered. Consideration of other models[8,15] leads us to conclude that Eq. (2.1) is satisfied as an equality (for $T>0$) if and only if a sufficient set of conjugate fields (i.e., conjugate to every possible phase of the system) has been introduced. Thus Eq. (2.1) can be used as a criterion for whether enough conjugate fields have been considered or not. It is noteworthy that Eqs. (1.1) and (2.1) depend only on topologically significant quantities like the dimension of a subspace in the phase diagram, and should therefore be understood as topological statements.

To illustrate the notation and to provide a good example of a system with a phase diagram exhibiting critical spaces of orders 2, 3, and 4, we consider the $d=3$ Ising model with variable interaction strength $\mathfrak{R}J$ between planes of constant z:

$$\mathcal{H}=-\sum_{x,y,z} S_{x,y,z}\left[J(S_{x+1,y,z}+S_{x,y+1,z}) + \mathfrak{R}JS_{x,y,z+1}+H+(-1)^z H_2\right]. \tag{2.2}$$

Here the symbol $S_{x,y,z}$ is the value of the spin on lattice site with coordinates (x, y, z). The variable $\mathfrak{R}$ allows for a variation in the strength of interaction in the z direction. The phase diagram of this model is four dimensional, with fields H, H_2, T, and the fieldlike variable $\mathfrak{R}$. For $\mathfrak{R}>0$, we have a three-dimensional Ising model with "lattice anisotropy," which tends as $\mathfrak{R}\to 0$ to the two-dimensional Ising model. The invariance of the Hamiltonian under the transformation $S_{x,y,z}\to(-1)^z S_{x,y,z}$, $\mathfrak{R}\to-\mathfrak{R}$, $H\to H_2$, and $H_2\to H$ relates the phase diagram for $\mathfrak{R}<0$ to that for $\mathfrak{R}>0$.

For $\mathfrak{R}<0$, Eq. (2.2) describes a metamagnet. The phase diagram of this system is well known and shown in Fig. 1. As $|\mathfrak{R}|$ is decreased, the values of T_t and T_N decrease (unpublished results

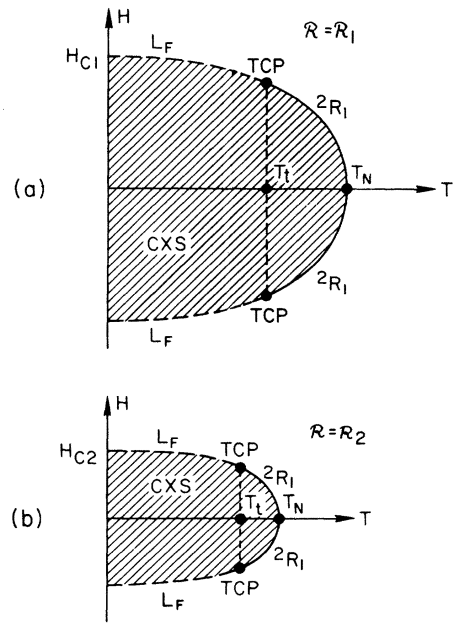

FIG. 1. (a) Phase diagram for $\mathcal{R}=\mathcal{R}_1<0$, in the (H, T) plane $(H'=0)$. The $^2R_1$ terminates at a pair of tricritical points ($^3R_0$) shown as TCP. The $^2X_2$ separating the antiferromagnetic phases A^+A^- is bounded below the tricritical temperature T_t by the lines of first-order transitions L_F, which terminate at a magnetic field value H_{C1}. (b) The same for $\mathcal{R}_2<0$, where $|\mathcal{R}_2|<|\mathcal{R}_1|$. Note that $H_{C2}<H_{C1}$ and that both T_t and T_N have decreased. See also, F. Harbus *et al.*, Ref. 1.

of F. Harbus). This is shown in the Fig. 1(b) as compared to Fig. 1(a).

As $|\mathcal{R}|\to 0$, the behavior of $T_N(\mathcal{R})$ is described by the well-known crossover exponent and symmetry between $\mathcal{R}<0$ and $\mathcal{R}>0$ mentioned above shows that in the plane $H=H_2=0$ there is a reflection symmetry about $\mathcal{R}=0$.

From these considerations we obtain Fig. 2, which is a three-dimensional phase diagram in the $H_2=0$ plane. For $\mathcal{R}<0$ and constant, there is a phase diagram like Fig. 1, and for $\mathcal{R}>0$ the ordinary crossover behavior holds.

The two tricritical points in Fig. 1 become lines of critical points of order 3, $^3R_1$, in Fig. 2. The symmetry of the Hamiltonian shows that there are two additional $^3R_1$ for $\mathcal{R}>0$ at nonzero H_2. The symmetry of the Hamiltonian forces these four lines (tricritical lines) to converge upon a point lying on the temperature axis—a critical point of order 4. On the temperature axis below the $^4R_0$ four phases are in coexistence: it is a $^4X_1$.

The validity of Eqs. (1.1) and (2.1) may be verified and it can also be seen that in this system a $^pX_{d+1}$ is bounded for increasing T by a $^{\mathcal{O}}R_d$, where $\mathcal{O}=p$. A CXS which in the full phase diagram is a $^pX_{d+1}$ is, when considered in the zero-temperature plane, only a ^pX_d. In the model considered in this section, therefore, a coexistence hypersurface which in the $T=0$ phase diagram is a ^pX_d evolves as the temperature increases into an $^{\mathcal{O}}R_d$, with $\mathcal{O}=p$. In other words, the space of critical points of order $\mathcal{O}$ is the upper bound (as temperature increases) of a space of points where $\mathcal{O}$ phases coexist.

This is a very significant point and can be understood by examples, and from the following consideration. In a phase diagram, a space where three phases coexist is necessarily a place of intersection of spaces where two phases coexist. The spaces where two phases coexist are bounded from above by spaces of critical points of order two. Therefore, the upper bound of the space where three phases coexist is either the boundary of one critical space of order 2 or the intersection of all three critical spaces of order 2. Because of the symmetry properties holding in the present model, and

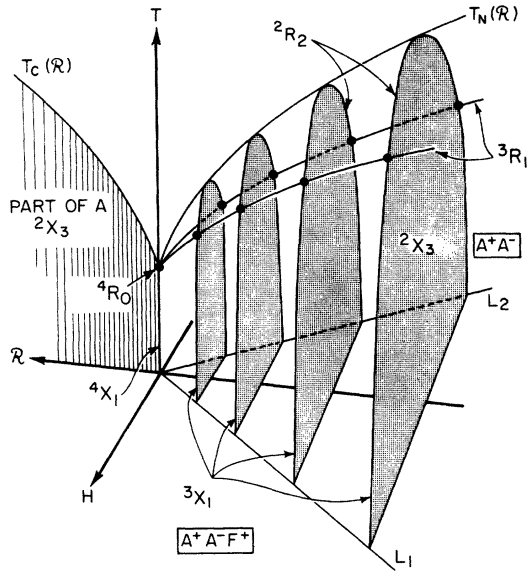

FIG. 2. Phase diagram in the $H_2=0$ hyperplane for Ising model with variable interplanar interaction. For $\mathcal{R}<0$ the $\mathcal{R}=$const sections are similar to Fig. 1. These sections are schematically shaded. As $\mathcal{R}$ varies continuously the ^pX_d and $^{\mathcal{O}}R_d$ of Fig. 1 become $^pX_{d+1}$ and $^{\mathcal{O}}R_{d+1}$. Thus the $^2X_2$ of Fig. 1 becomes the interior of the "mountain"; this is a $^2X_3$ separating phases A^+, A^-. The lines L_F where three phases coexist become surfaces of the mountain ($^3X_2$) below the line of tricritical points $^3R_1$ corresponding to TCP of Fig. 1. The $^2R_1$ of Fig. 1 becomes a $^2R_2$, the top of the "mountain" in Fig. 2. The T axis becomes a line of special points where all four phases A^+, A^- and the ferromagnetic F^+ and F^- all coexist; it is a $^4X_0$. The $^3R_1$ meet at the T axis at the end of this line; at a $^4R_0$. The region $\mathcal{R}>0$ appears simpler because it corresponds to the $(H=0)$ section of $\mathcal{R}<0$, and the rest of the mountain occurs at $H_2\neq 0$. See also, F. Harbus *et al.*, Ref. 1.

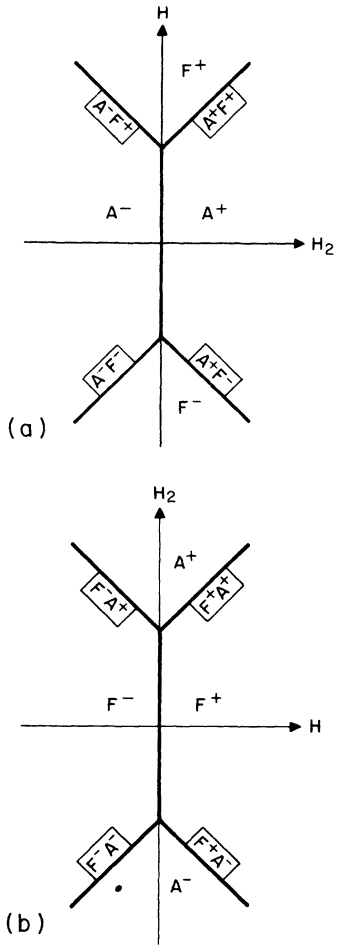

FIG. 3. The phase diagram at $T=0$ of an Ising (a) antiferromagnet and (b) ferromagnet. The phases with spins parallel are indicated by $F^{\pm}$ and with spins antiparallel by $A^{\pm}$. The lines indicate where the various phases are in equilibrium.

also because it is an Ising model, the latter condition holds. An entirely analogous argument can be constructed for critical points of order 4 or more.

It is therefore possible, for Ising models, to make predictions about the relationships between ${}^{6}R_d$ in the full phase diagram, by considering the relationships between the ${}^{p}X_d$ in the $T=0$ phase diagram. We will make extensive use of this method in Sec. III.

III. SPACES OF TRICRITICAL POINTS IN ONE-DIMENSIONAL MODELS

There has been much work recently on one-dimensional Ising models possessing a long-range interaction.[8,15] The effect of this interaction is to shift the critical temperature from the value $T=0$ to a nonzero temperature, thereby enabling the critical points to obey scaling laws.

The purpose of this section is to display two models for which critical points of order $\mathcal{O}=4$ occur; these are both Ising models with long-range interactions.[16]

Models exhibiting a critical point of order 4 also possess a line of points where four phases coexist, as explained at the end of Sec. II. Therefore, a simple method of deciding whether a particular model can possess a critical point of order 4 is to analyze the $T=0$ hyperplane of the phase diagram and see if points where four phases coexist continue to have four distinct phases in equilibrium as T is increased. Cases where this does and does not happen are discussed below.

Before analyzing a case where there is a long-range interaction, let us consider the $T=0$ phase diagram of a one-dimensional Ising antiferromagnet with only nearest-neighbor interactions.

Hamiltonians

The Hamiltonian is given by

$$\mathcal{H}_{SR}=-J_{SR}\sum_{i=1}^{N-1}s_i s_{i+1}-H\sum_{i=1}^{N}s_i-H_2\sum_{i=1}^{N}(-)^{i+1}s_i\,, \tag{3.1}$$

where J_{SR} is the nearest-neighbor (nn) interaction strength and $s_i=\pm 1$ are the Ising spins situated at site i of the chain. When $J_{SR}>0$ the interaction is ferromagnetic and when $J_{SR}<0$ the interaction is antiferromagnetic. H is the magnetic field and H_2 is the staggered magnetic field of wavelength 2 lattice sites. The phase diagram will appear as in Fig. 3(a). Here the four phases $F^{\pm}$, $A^{\pm}$ are defined in Table I: F means ferromagnetic and A means antiferromagnetic. The $T=0$ "critical point" of the

TABLE I. Definitions, energies, and equations of Figs. 3 and 5. Here $\tilde{\mathfrak{R}}\equiv J_{SR}/J_{LR}$; $h\equiv H/J_{LR}$; $h_2\equiv H_2/J_{LR}$. Star means not shown in Fig. 5.

Configuration	Name	Field	Energy
↑ ↑	F^+	H	$E_F=-J_{LR}-J_{SR}-H$
↓ ↓	F^-		
↑ ↓	A^+	H_2	$E_2=+J_{SR}-H_2$
↓ ↑	A^-		

Surface	Equation	Line	Equation
$[F^+,F^-]$	$H=0$	L_1	$h_2=1+2\tilde{\mathfrak{R}};\ h=0$
			$\tilde{\mathfrak{R}}>-\frac{1}{2}$
$[A^+,A^-]$	$H_2=0$	L_2	$h_2=1-2\tilde{\mathfrak{R}};\ h=0$
$[F^+,A^+]^*$	$h-h_2+1+2\tilde{\mathfrak{R}}=0$	L_3	$h=-1-2\tilde{\mathfrak{R}};\ h_2=0$
			$\tilde{\mathfrak{R}}<-\frac{1}{2}$
$[F^-,A^-]^*$	$h-h_2-1+2\tilde{\mathfrak{R}}=0$	L_4	$h=-1+2\tilde{\mathfrak{R}};\ h_2=0$
$[F^+,A^-]^*$	$h+h_2+1+2\tilde{\mathfrak{R}}=0$		
$[F^-,A^+]^*$	$h+h_2-1-2\tilde{\mathfrak{R}}=0$		

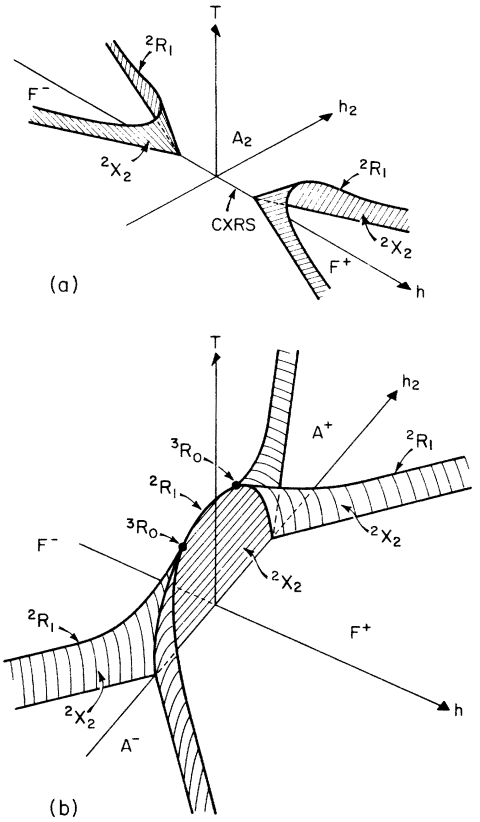

FIG. 4. (a) The extension of Fig. 3(a) into the space with $T>0$ when a weak long-range interaction is included. Note that the $T=0$ plane corresponds to Fig. 3(a), and that the $[A^+,A^-]$ phase boundary only separates phases at $T=0$. The other lines in Fig. 3(a) develop normally, giving coexistence surfaces ($^2X_2$) ending in critical lines $^2R_1$. (b) The phase diagram of the same model but without the antiferromagnetic interaction ($J_{SR}=0$ or $J_{SR}>0$). Now all lines in the $T=0$ plane become coexistence surfaces $^2X_2$. The points of interaction become $^3X_1$ (lines where three phases coexist) and there terminate at two $^3R_0$ (tricritical points).

Ising antiferromagnet becomes a *line* of critical points for nonzero values of magnetic field. This line bifurcates at points where it is energetically more favorable[17] for the system to order ferromagnetically (i.e., with all spins parallel).

Normal scaling laws do not apply to one-dimensional Ising models with short-range interactions, as these display essential singularities at the $T=0$ critical point. Thus the lines in Fig. 3(a) are lines of both critical points and coexistence points. These lines do not have very much in common with either the conventional critical points ^2R_d or the conventional coexistence surfaces ^pX_d that divide up the field space at finite values of temperature. A suitable nomenclature for the lines of Fig. 3(a) might be "coexistence-critical surfaces" and we will denote them by CXRS. A CXRS is necessarily confined to the $T=0$ plane as for Fig. 3(a). Thus we see that the nn Ising antiferromagnet contains five CXRS lines where two phases coexist and two CXRS points where three phases coexist.

Then we introduce in addition to $\mathcal{H}_{SR}$ of Eq. (3.1), a long-range interaction, defined by the Hamiltonian

$$\mathcal{H}_{LR}=-\sum_{i=1}^{N}\sum_{r}J(r)s_i s_{i+r}, \tag{3.2a}$$

where

$$J(r)=\lim_{\gamma\to 0} a\gamma e^{-\gamma|r|}, \tag{3.2b}$$

the phases $F^{\pm}$ are stabilized at nonzero temperature and continue to show long-range order for $T>0$. The phase diagram is given in Fig. 4(a). The CXRS [on the H axis of Fig. 3(a)] is not stabilized at $T>0$ by the long-range interaction; the two antiferromagnetic phases $A^{\pm}$ coexisting at the CXRS at $T=0$, simply become a single disordered phase for $T>0$.

There are two $^2X_2$ separating the ordered (ferromagnetic) phase from the disordered phase at higher temperatures. These $^2X_2$ end in $^2R_1$ (lines of critical points).

If the dominating nearest-neighbor interactions are ferromagnetic, $J_{SR}>0$, then the situation depicted in Figs. 3(b) and 4(b) results. The two points where three phases coexist at $T=0$ become the end points of two $^3X_1$ lines where three phases coexist. Each $^3X_1$ line terminates at a $^3R_0$ (a tricritical point).

If sufficient care is taken to decide whether a space in the $T=0$ hyperplane is a CXRS or a CXS, then the nature of the extension of the space and its subspaces into $T>0$ can be easily ascertained. The rules exemplified from Figs. 3 and 4 are the following: (i) Two phases which can only be distinguished by a staggered magnetic field coexist on a CXRS. (ii) Such staggered phases give only one phase for $T>0$. (iii) A line where one phase which maintains order for $T>0$ coexists with any other phase is *always* a CXS. (iv) A point where a CXRS meets a CXS has no special properties. It is simply a point on a CXS.

Using these rules we can analyze the model of Nagle and Bonner[8] which includes a long-range interaction, a variable short-range interaction, and the two fields of Fig. 3.[18] A point where four critical lines meet, a tetracritical point, is known for this model. We will show here that this point is a critical point of order 3. Since a variant of this model, which we discuss below, shows a critical point of order 4, it is worth treating the Nagle-Bonner model in some detail first.

Figure 5 depicts the surfaces of coexistence of the four phases in the $T=0$ plane. Definitions and

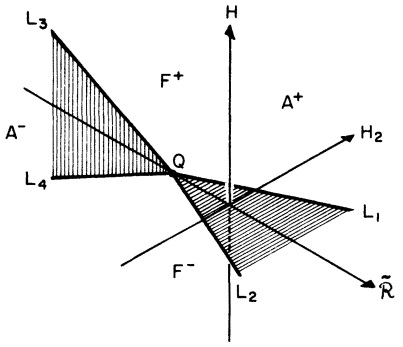

FIG. 5. $T=0$ hyperplane for an Ising model with competing long- and short-range interactions. Here $\tilde{\mathcal{R}} \equiv J_{SR}/J_{LR}$ and H_2 is a staggered magnetic field of wavelength 2 lattice sites. The lines L_1, L_2 are in the $(H_2, \tilde{\mathcal{R}})$ plane, and the lines L_3, L_4 are in the $(H, \tilde{\mathcal{R}})$ plane. The surfaces $[A^-F^+]$, $[A^+F^-]$, $[F^+,A^+]$, $[F^-,A^-]$ have been omitted. The surface $[A^+,A^-]$ is a CXRS, Fig. 3(a) is an (H_2, H) plane for $\tilde{\mathcal{R}}<\tilde{\mathcal{R}}_Q$, while Fig. 3(b) is for $\tilde{\mathcal{R}}>\tilde{\mathcal{R}}_Q$.

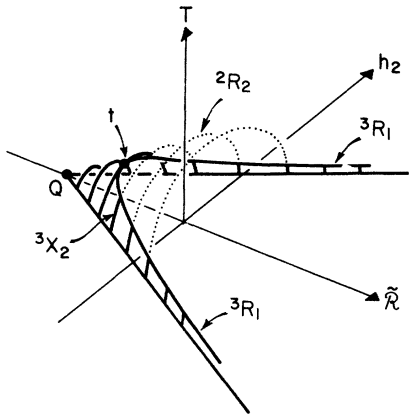

FIG. 6. $H=0$ hyperplane of the model of Fig. 5. The lines L_1, L_2 extend into $T>0$. The lines where three phases coexist in Fig. 4(b) have become a single surface, denoted here by $^3X_2$. This terminates at a *line* of tricritical points $^3R_1$; the $^3R_1$ also bounds a surface of ordinary critical points $^2R_2$. The point t where the $^3R_1$ intersects the plane $h_2=0$ is the location of the tetracritical point (Ref. 8). The $\tilde{\mathcal{R}}=0$ section of this figure corresponds to the $H=0$ section of Fig. 4(b). Note that at t a surface $\tilde{\mathcal{R}}=$const is parallel to the $^3R_1$.

equations are given in Table I. For clarity four surfaces are omitted; e.g., those that separate the phases $[F^+A^+]$, $[F^-A^-]$, $[F^+A^-]$, and $[F^-A^+]$. As may be seen there are four lines where three phases coexist and a point Q where all four phases coexist. The surface $[A^+A^-]$ bounded by the lines L_3, L_4, is a CXRS since for constant values of $\tilde{\mathcal{R}}$ less than x_Q, the phase diagrams are the same as Figs. 3(a) and 4(a). Here

$$\tilde{\mathcal{R}} \equiv J_{SR}/J_{LR} \,, \tag{3.3}$$

where J_{LR} is the "equivalent neighbor" long-range parameter.[8]

For $T\neq 0$, the two $^2X_2$ surfaces $[A^+F^+]$ and $[A^-F^-]$ of Fig. 5 end in a single surface of critical points, and the same is true for the $[A^-F^+]$, $[A^+F^-]$ surfaces; this is shown in Fig. 4(a). The point Q of Fig. 5, where four phases coexist,

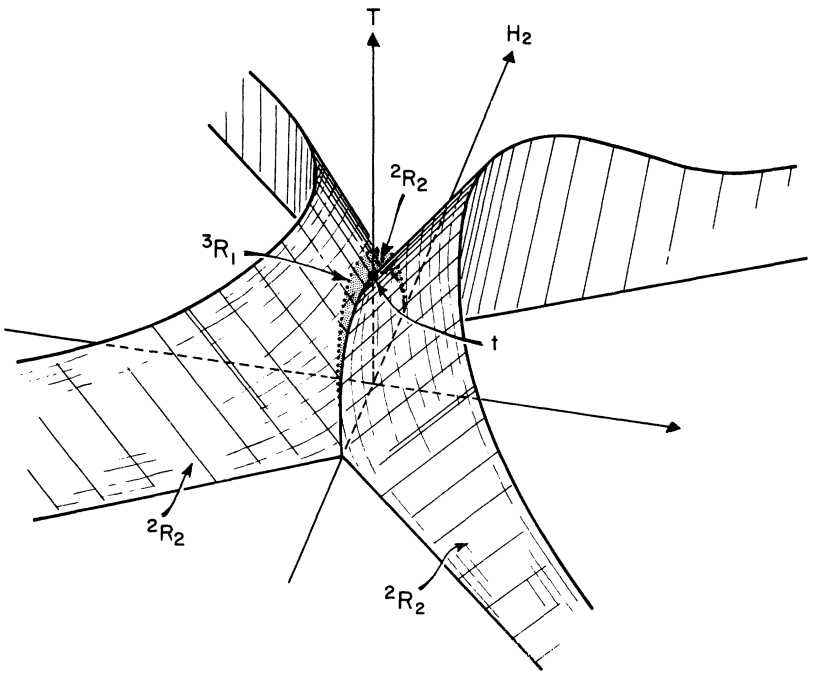

FIG. 7. Ray projection of the four-dimensional space, from Q onto $\tilde{\mathcal{R}}=0$ showing the topology of the surfaces of critical points. The $\tilde{\mathcal{R}}$ axis in Figs. 5 and 6 has become a combination of $\tilde{\mathcal{R}}$ and h. The curved $^2R_2$ surfaces are the ends of those surfaces which end on L_3 and L_4 of Fig. 5. The $^2R_1$ of Figs. 4(a) and 4(b) are lines in this surface. The flat $^2R_2$ shown in the (T, H_2) plane is the surface $^2R_2$ of Fig. 6.

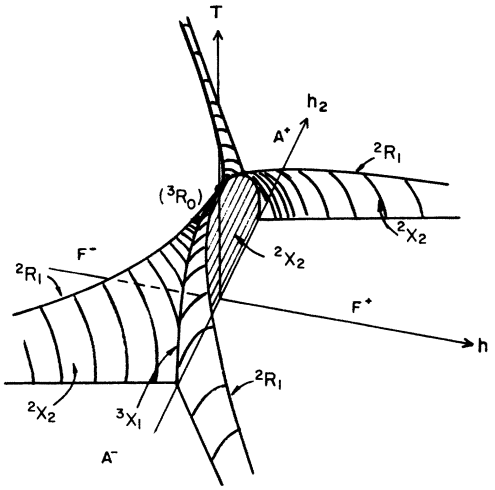

FIG. 8. Plot of the ${}^2X_2$ and the four lines of critical points meeting at the tetracritical point t. The value of the interaction strength ratio $\tilde{\mathcal{R}} \equiv J_{SR}/J_{LR}$ is equal to its appropriate value $\tilde{\mathcal{R}}_c = 0$.

is seen (Fig. 6) to be only a special point on a ${}^3X_2$ and Q does *not* give rise to a ${}^4X_1$ on increasing the temperature. To see this (in the full phase diagram) it is necessary to consider Figs. 4(b) and 5–7. First, in Fig. 4(b), the phase diagram of the system is shown at constant $\tilde{\mathcal{R}} > 0$. The relationship of this figure to Fig. 5 can be understood by looking at the $T = 0$ plane of Fig. 4(b). The lines where two phases coexist are lines on the appropriate surfaces of Fig. 5, and points where lines in the $T = 0$ plane of Fig. 4(b) meet are points on the lines L_1, L_2. Therefore Fig. 4(b) shows that the lines L_1, L_2 do give rise to coexistence surfaces and are lines on ${}^3X_2$, as shown in Fig. 6. The line of points where three phases coexist (${}^3X_1$) in Fig. 5 has become a surface (${}^3X_2$) in Fig. 6, and this surface is terminated by a single line of tricritical points, ${}^3R_1$. Figure 6 shows that the point Q is just a point on a ${}^3X_2$, and does not generate a ${}^4X_1$.

The three surfaces of critical points generated by the lines of critical points in Figs. 4(a) and 4(b) are shown schematically in Fig. 7. It can be seen that the two ${}^3R_0$ (tricritical points) of Fig. 4(b) form a continuous line (a ${}^3R_1$) bounding three ${}^2R_2$ (surfaces of critical points). The point t was called a tetracritical point by Nagle and Bonner[8] because, for $\tilde{\mathcal{R}} = \tilde{\mathcal{R}}_c$, *four* lines of critical points meet there (see Fig. 8). However, Figs. 6 and 7 show that t is an indistinguishable point on a smooth line of tricritical points of order 3; this is corroborated by the fact[8] that the exponents at t are the same as at the other tricritical points.

To produce a model where the point Q is stable at higher temperatures demands only a slight change in the structure of the interactions. We draw the linear-chain nearest-neighbor Ising antiferromagnet in the form shown in Fig. 9, with the nn antiferromagnetic interaction along the solid lines, and a long-range interaction along each of the dotted lines. The latter stabilizes each sublattice independently, enabling the system to adopt an antiferromagnetic ordering at nonzero temperature:

$$\mathcal{H}_i = \mathcal{H}_{SR} + \mathcal{H}^0_{LR} + \mathcal{H}^E_{LR}, \tag{3.4a}$$

where

$$\mathcal{H}^{0,E}_{LR} = -\sum_i \sum_r J(2r) s_i s_{i+2r}. \tag{3.4b}$$

Here odd-numbered spins are on the top lattice of Fig. 9 and $\mathcal{H}^0$ has all i odd. Even numbered spins are on the lower lattice and $\mathcal{H}^E$ has all i even; $J(2r)$ is defined by Eq. (3.2b). The point Q is now at the origin and stable for $T > 0$, and we are able to have four ${}^3X_2$; these are generated by the lines L_1, L_2, L_3, L_4 (of Fig. 5) meeting at the ${}^4X_1$, generated by Q. The ${}^3X_2$ should end in a ${}^3R_1$ (as in Fig. 6) but unlike the system of Fig. 6, the ${}^3R_1$ all terminate at a ${}^4R_0$.

This Hamiltonian has an important discrete symmetry which will necessarily be reflected by the phase diagram of the solution of the model. It is given by the operation $s_i \to (-)^i s_i$, $H \to H_2$, $H_2 \to H$, $J_{SR} \to -J_{SR}$. Therefore,

$$G(H, H_2, T; +J_{SR}) = G(H_2, H, T; -J_{SR}).$$

Further, the point Q in Fig. 5 (which is now stable at $T > 0$) is now located at the origin. There are now four ${}^3R_1$; two of which lie in the $H_2 = 0$ hyperplane for $\tilde{\mathcal{R}} < 0$ and these are symmetrically complemented by two more ${}^3R_1$ in the $H = 0$ for $\tilde{\mathcal{R}} > 0$. These four ${}^3R_1$ meet at the T-axis at some finite value of T. This point at which all four ${}^3R_1$ meet is a ${}^4R_0$. The phase diagram for this model is the same as that for the Ising model with variable interplanar interaction discussed in Sec. II (Figs. 1 and 2).

For the model just discussed, we were able to make use of the extensive analysis of Nagle and Bonner in conjunction with the $T = 0$ phase diagram, and thus we deduced the structure of the full phase diagram. The existence of the discrete symmetry and the consequent analogy with the model discussed in Sec. II makes us more confident in our conclusions.

For the next model, we use only an analysis of the $T = 0$ phase diagram and we make the extrapola-

FIG. 9. Modified one-dimensional lattice exhibiting a critical point of order $\Theta = 4$. The solid lines represent antiferromagnetic interactions and the dashed lines, long-range (ferromagnetic) interactions.

TABLE II. Definitions of spin orderings of phases and fields for an Ising model with two staggered fields.

Spin configuration	Name	Conjugate field
↑ ↑ ↑ ↑	F^+	H
↓ ↓ ↓ ↓	F^-	
↑ ↓ ↑ ↓	A_2^+	H_2
↓ ↑ ↓ ↑	A_2^-	
↑ ↑ ↓ ↓	A_4^+	H_4
↓ ↓ ↑ ↑	A_4^-	
↑ ↑ ↑ ↓	M_a^+	$\frac{1}{2}[H_2+H_4\pm H]$
↑ ↓ ↓ ↓	M_a^-	
↑ ↑ ↓ ↑	M_b^+	$\frac{1}{2}[-H_2+H_4\pm H]$
↓ ↑ ↓ ↓	M_b^-	
↑ ↓ ↑ ↑	M_c^+	$\frac{1}{2}[H_2-H_4\pm H]$
↓ ↓ ↑ ↓	M_c^-	
↓ ↑ ↑ ↑	M_d^+	$\frac{1}{2}[-H_2-H_4\pm H]$
↓ ↓ ↓ ↑	M_d^-	

tions explained at the end of Sec. II. Our knowledge of the extensive occurrence of tricritical points in certain Ising models gives us a reasonable basis from which to predict the existence of a critical point of order 4.

This second model for which an exact solution is fairly readily obtainable[18] is a model with a second staggered magnetic field. It turns out that the analysis for an exact solution is simplest if the staggered field, "H_4," is of wavelength four lattice sites.[19] The Hamiltonian will therefore be given by

$$\mathcal{H}=\mathcal{H}_{\rm SR}+\mathcal{H}_{\rm LR}-H_4\sum_{i=1}^{N}u_i s_i\,, \tag{3.5}$$

where the number $u_i=+1$ for $i=4n+1$, $4n+2$ and $u_i=-1$ for $i=4n-1$, $4n$. We define the names of the various phases in Table II and also the phase of H_4 relative to H_2. We give the energies of the phases at $T=0$ in Table III. The phase adopted at $T=0$ is that of lowest energy, and so the problem of finding the phase diagram at $T=0$ is simple. The phases coexist at points where the energies of two different phases are equal, and the most important equalities are given in Table IV(a).

An extended analysis[16] shows that the significant values of $\tilde{\mathcal{R}}$ are -1, $-\frac{1}{2}$, and 0, and a sequence of phase diagrams can be drawn in the space of variables H, H_2, H_4 for values of $\tilde{\mathcal{R}}$ greater than, equal to, and less than these numbers. A representative

TABLE III. Energies of various phases at $T=0$ for an Ising model with two staggered fields. Here the long-range energy is given by $J_{\rm LR}$ and the nearest neighbor by $J_{\rm SR}$. Only the phase + is shown; to get the value of E_{X^-}, reverse the sign of the conjugate field.

Phase	Energy per spin
F^+	$E_F=-J_{\rm LR}-J_{\rm SR}-H$
A_2^+	$E_2=+J_{\rm SR}-H_2$
A_4^+	$E_4=-H_4$
M_a^+	$E_a=-\frac{1}{2}J_{\rm LR}-\frac{1}{2}[+H_2+H_4+H]$
M_b^+	$E_b=-\frac{1}{2}J_{\rm LR}-\frac{1}{2}[-H_2+H_4+H]$
M_c^+	$E_c=-\frac{1}{2}J_{\rm LR}-\frac{1}{2}[+H_2-H_4+H]$
M_d^+	$E_d=-\frac{1}{2}J_{\rm LR}-\frac{1}{2}[-H_2-H_4+H]$

TABLE IV. (a) Equations of planes and lines in Fig. 10 for an Ising model with two staggered fields. Here we have divided all energies through by $J_{\rm LR}$ and defined $h_i=H_i/J_{\rm LR}$, $\tilde{\mathcal{R}}\equiv J_{\rm SR}/J_{\rm LR}$. In Fig. 10, $\tilde{\mathcal{R}}$ is positive, e.g., $\frac{1}{2}$ or ∞. Star means that the plane was omitted from Fig. 10. Double star indicates that this is only a line: (b) Equations of lines in Fig. 10.

(a)

Phase boundary	Equation	Region
$[F^+,F^-]$	$h=0$	
$[M_a^+,M_a^-]$	$h=0$	
$[F^+,M_a^+]^*$	$h_2+h_4-1-2\tilde{\mathcal{R}}=h$	$h,h_2,h_4>0$
$[F^+,M_b^+]^*$	$h_2-h_4+1+2\tilde{\mathcal{R}}=-h$	$h,h_4>0,\ h_2<0$
$[F^+,A_4^+]$	$h_4-1-\tilde{\mathcal{R}}=h$	$h_4>0,\ h>0$
$[A_4^+,M_a^+]$	$h_4-h_2-1=h$	$h,h_4>0,\ h_2>0$
$[A_4^+,M_b^+]$	$h_4+h_2-1=h$	$h,h_4>0,\ h_2<0$
$[F^+,A_2^+]^{**}$	$h_2-1-2\tilde{\mathcal{R}}=h$	$h,h_2>0;\ h_4=0$
$[A_2^+,M_a^+]$	$h_2-h_4-1-2\tilde{\mathcal{R}}=h$	$h,h_2,h_4>0$

(b)

Line	Intersection	Equation
$[4:F^+F^-M_a^+M_a^-]$	$[F^+,F^-]\,[M_a^+,M_a^-]$	$h_2+h_4=1+2\tilde{\mathcal{R}}$
	$[F^+,M_a^+],\,[F^-,M_a^-]$	$h=0$
$[3:F^+F^-A_4^+]$	$[F^+,F^-]\,[F^+,A_4^+]$	$h_4=1+\tilde{\mathcal{R}}$
	$[F^-,A_4^+]^*$	$h=0$
$[3:F^+M_a^+A_4^+]$	$[F^+,A_4^+]\,[A_4^+,M_a^+]$	$h_4-h=1+\tilde{\mathcal{R}}$
	$[F^+,M_a^+]^*$	$h_2=\tilde{\mathcal{R}}$
$[3:F^+M_b^+A_4^+]$	$[F^+A_4^+]\,[A_4^+,M_b^+]$	$h_4-h=1+\tilde{\mathcal{R}}$
	$[F^+,M_b^+]^*$	$h_2=-\tilde{\mathcal{R}}$
$[4:F^+M_a^+M_c^+A_2^+]$	$[F^+,M_a^+]^*[F^+M_c^+]^*$	$h_2-h=1+2\tilde{\mathcal{R}}$
	$[M_a^+,A_2^+]\,[M_c^+,A_2^+]$	$h_4=0$
$[3:M_a^+,M_a^-,A_4^+]$	$[M_a^+,M_a^-]\,[M_a^+,A_4^+]$	$h_4-h_2=1$
	$[M_a^-,A_4^+]^*$	$h=0$
$[3:M_a^+,M_a^-,A_2^+]$	$[M_a^+,M_a^-],\,[M_a^+,A_2^+]$	$h_2-h_4=1+2\tilde{\mathcal{R}}$
	$[M_a^+,A_2^-]$	$h=0$

diagram is shown in Fig. 10 for which the equations of the lines are given in Table IV(b). Some of the surfaces and lines of Fig. 10 are labeled and the reader can discover the labels for the rest by reference to Tables IV(a) and IV(b).

There are several important points about this model: firstly, the "mixed" phases $M_a^{\pm}$ are distinguished at $T=0$ as $M_a^+ \cdots M_d^+$ but above absolute zero there are only phases M^+ and M^-. The phases $M^{\pm}$ are stable for $T>0$ because they contain a long-range contribution to their energy; thus all the lines and surfaces on Fig. 10 will survive at $T>0$ because they separate phases stabilized by the long-range interaction from phases $(A_2^{\pm}, A_4^{\pm})$ stable only at $T=0$.

There are several points where many phases coexist. In particular, at the point P_2 the phases $F^{\pm}$, $M_a^{\pm}$, and A_4^+ coexist. The lines where three or more phases coexist which meet at P_2 are all stable at $T>0$ and so should end in tricritical points. Thus P_2 will give rise to a line of points where five phases coexist; this line ends at a critical point of order 4. Other points in Fig. 10 (viz., P_1) are much more complex in structure and will not be discussed here. The object of introducing the model given by Eq. (3.5) was to show a critical point of order four and this, at least, we have done.

In this section we have shown that it is reasonably easy to find model systems which are soluble and which show critical points of order 4 or more. The analysis of the two models suggested was omitted for the sake of brevity, and will be given in future work.[16]

IV. SPECIAL DIRECTIONS AT CRITICAL SPACES OF ORDER Θ: A SET OF "CANONICAL DIRECTIONS"

In order to properly formulate the scaling hypothesis for multicomponent systems, it is important to choose the proper independent variables. It is this problem that is treated in the present section. We shall argue that the considerations that Griffiths and Wheeler[5] applied to their discussion of second-order critical spaces $({}^2R_d)$ can be extended to spaces of higher order in a natural and straightforward fashion.

A ${}^2X_d$ is, by definition, a hypersurface where two phases coexist; it necessarily divides the total space of n field variables locally into two regions and is therefore of dimension $d=n-1$, where n is the total number of truly intensive or "field" variables.[5] A ${}^2R_d$ (a simple second-order critical space) is the boundary of a ${}^2X_{n-1}$ and is therefore of dimension $d=n-2$.

At a ${}^2R_{n-2}$ there are $n-2$ directions parametrizing the critical space. The two remaining directions are of significance for the generalized scaling hypothesis. Directions not locally parallel to the ${}^2X_{n-1}$ (coexistence surface) we call strong directions, and directions locally parallel to the ${}^2X_{n-1}$ but not in the ${}^2R_{n-2}$ we call weak directions. The strong and weak directions will be called directions of type 1 and 2, respectively; this terminology is useful in Sec. VI and in Paper II, where the appropriate generalization to critical spaces of order larger than 2 is made. Examples are given in Figs. 11 and 12.

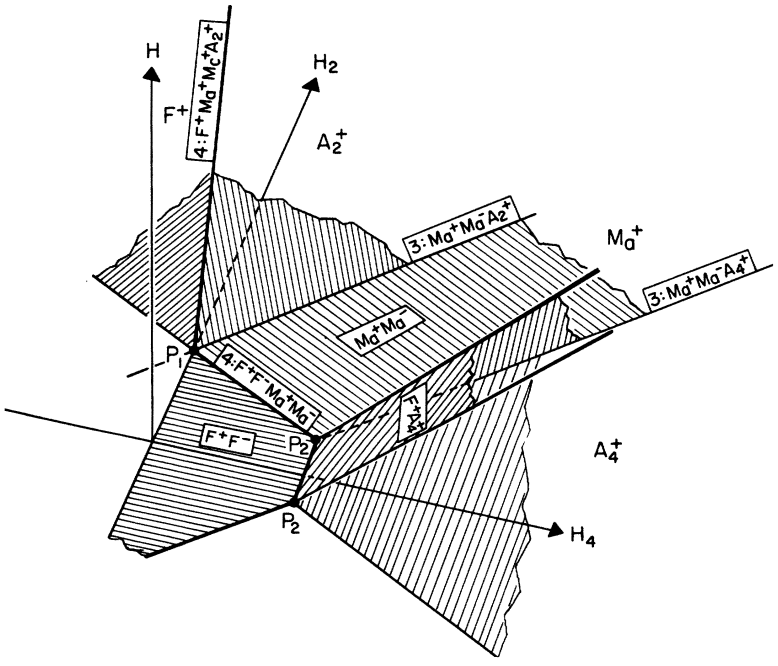

FIG. 10. Coexistence surfaces in the $T=0$ phase for a system with a long-range interaction, a nn interaction, magnetic field h, and staggered magnetic fields h_2, h_4 of wavelengths 2 and 4. Here the short-range interaction is also ferromagnetic. The surfaces are labeled by the phases in coexistence. The surface $[F^+, M_a^+]$ is omitted. The lines are labeled by the three or four phases in coexistence there. At the point P_2, five phases coexist; at P_1, seven phases coexist. The phases F and M are stable above $T=0$.

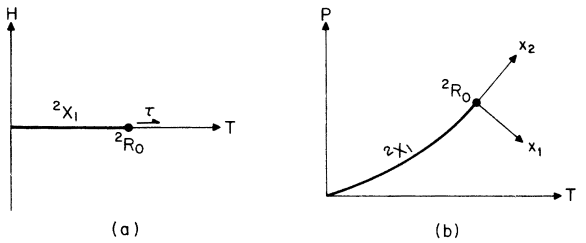

FIG. 11. (a) Phase transition for a ferromagnetic system. The coexistence surface $^2X_1$ ends at a critical point $^2R_0$. The strong direction H and weak direction τ are defined at the $^2R_0$. (b) Phase transition for a simple fluid. The coexistence surface $^2X_1$ ends at a critical point $^2R_0$. The strong direction x_1 and weak direction x_2 are indicated; both P and T directions are strong.

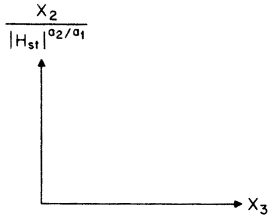

FIG. 13. Invariant space for an antiferromagnet. (x_3 is merely a parameter.)

Next, we introduce the concept of a direction of type 3. In the examples discussed, the critical spaces of order 3 have a dimension of $d=n-3$. If one approaches a particular tricritical point along a line of critical points of order 2, then in addition to the two directions singled out by the $^2R_1$ (and its associated $^2X_2$), there is a third direction of significance for scaling. This direction, which we call a direction of type 3, is a direction tangent to the line of critical points (Figs. 12 and 14). This concept is easily generalized to $n>3$ for the case mentioned above, for which the dimension d of the space of critical points of order three is indeed given by $d=n-3$. In this case directions of type 3 are those directions which are neither strong nor weak for a particular $^2R_{n-2}$ bounded by the $^3R_{n-3}$, nor are they locally tangent to the space of critical points of third order.

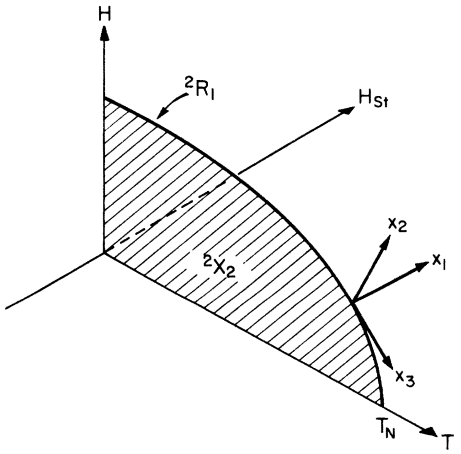

FIG. 12. Phase transition for an antiferromagnet. The coexistence surface $^2X_2$ lies in the H, T plane and the line of critical points $^2R_1$ bounds it. The strong direction is everywhere H_{st}, the staggered magnetic field. The weak direction may be either H or T, *except* at the Néel point where it can only be T. The independent direction x_0 lies in the $^2R_1$.

In the similar cases where Eq. (1.1) holds as an equality, one can generalize the above concepts to define directions of types 1, 2, ..., $\mathfrak{o}$, and these are important in applying the scaling hypothesis to critical spaces of order $\mathfrak{o}$. Specifically, since a critical point of order $\mathfrak{o}$ is, by definition, a particular point on a "line" of critical points of order $\mathfrak{o}-1$, the generalization follows by analogy with the case treated above. The directions of types 1 through $\mathfrak{o}$ are of great importance because they are used as the independent variables of the Gibbs function when the scaling hypothesis is made. Accordingly, they will be referred to in later sections as the "principal directions of scaling."

Thus, to set up a coordinate system at a $^{\mathfrak{o}}R_{n-\mathfrak{o}}$ (a general critical space of order $\mathfrak{o}$), a set of critical spaces $^jR_{n-j}$ of orders $j=2, 3, \ldots, \mathfrak{o}$ must be selected. This set of spaces must satisfy an inclusion principle: $^{\mathfrak{o}}R_{n-\mathfrak{o}} \subset {}^iR_{n-i} \subset {}^jR_{n-j}$ for $j<i<\mathfrak{o}$. The directions of types 1, 2, ..., $\mathfrak{o}$ are then sequentially defined. Here the inclusion symbol $\subset$ means not only that the $^iR_{n-i}$ is also part of a $^jR_{n-j}$ (for $i>j$) but also that the $^iR_{n-i}$ can be reached as a limiting point or boundary of the $^jR_{n-j}$.

The hierarchy of spaces $^jR_{n-j}$ is not unique, and the large number of choices available presents an apparent problem because many more than $\mathfrak{o}$ linearly independent vector directions are definable. For the $\mathfrak{o}=3$ example of Fig. 14 the $^3R_0$ can be approached along any of the three $^2R_1$, and each of these three "critical lines" (with its associated $^2X_2$) defines a set of directions of types 1, 2, and 3. This apparent problem is resolved by the generalized scaling hypothesis, because the shape of each critical space of order j ($j<\mathfrak{o}$) near the $^{\mathfrak{o}}R_d$ is constrained by the scaling hypothesis so that all the different directions end up mutually consistent. Accordingly, we now turn our attention to the scaling hypothesis, making it firstly in Sec. V for simple systems ($n=2$), for $n=3$ systems with a $^3R_0$ (tricritical point) in Sec. VI, and in Paper II for a $^{\mathfrak{o}}R_{n-\mathfrak{o}}$ (a general critical space of order $\mathfrak{o}$).[20]

V. INVARIANT THEOREMS OF ONE-PARAMETER CONTINUOUS GROUPS; APPLICATION TO THE SCALING HYPOTHESIS FOR CRITICAL SPACES OF ORDER 2

The scaling hypothesis for a simple system with two independent field variables can be made in

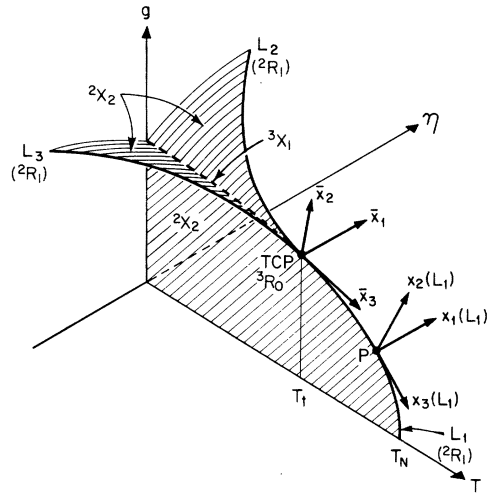

FIG. 14. Phase diagram for a metamagnet. The three $^2X_2$ end in lines of critical points $^2R_1$. These lines intersect at the tricritical point $^3R_0$. At a point P on the line L_1, a triad of strong, weak, and parallel (to L_1) directions is shown. This triad attains the limiting orientation $(\bar{x}_1, \bar{x}_2, \bar{x}_3)$ at the tricritical point $^3R_0$.

several essentially equivalent fashions. One statement is that the singular part of the Gibbs potential is asymptotically a generalized homogeneous function (GHF) of the appropriate variables.[21] For the simple magnet, this statement takes the form that there exist two numbers a_H, a_τ (called "scaling powers") such that for all positive λ,

$$G(\lambda^{a_H}H, \lambda^{a_\tau}\tau) = \lambda G(H, \tau), \tag{5.1}$$

where H is the magnetic field and $\tau \equiv T - T_c$. Using Eq. (5.1), one can express all possible thermodynamic exponents in terms of (a_H, a_τ).[21]

This form of the scaling hypothesis implies that the singular part of the Gibbs potential

$$G = F(H, \tau) \tag{5.2}$$

is an invariant equation under the "scaling" transformation defined by

$$G' \equiv \lambda G, \tag{5.3a}$$

$$H' \equiv \lambda^{a_H}H;\ \tau' \equiv \lambda^{a_\tau}\tau, \tag{5.3b}$$

such that $G' = F(H', \tau')$. The transformations defined by Eq. (5.3) form a one-parameter group[22] $\mathcal{G}_F$ and the scaling hypothesis may be restated in the following fashion: (5.2) is an invariant equation under the group of transformations $\mathcal{G}_F$ of (5.3).

For a simple magnet the thermodynamic axes are parallel to the directions used in the scaling hypothesis (5.1) (the "principal axes of scaling"). In other systems, this is not always so. In Fig. 11 we contrast the phase diagrams of a simple fluid and a simple magnet, and show the orientations of the strong and weak directions (x_1, x_2) for each. For a magnet, H is a strong direction and τ is the weak direction, but Fig. 11(b) shows that for a simple fluid, both P *and* T are strong directions and that the weak direction, x_2, is a special combination of the P and T directions.

This is usually the case for general thermodynamic systems—more than one thermodynamic axis is strong (as for the simple fluid) or more than one axis is weak (as for an antiferromagnet, see Fig. 12).

The scaling hypothesis at a $^2R_{n-2}$ for a general system can be made by choosing the strong and weak directions as the principal axes of scaling. Then the statement is that the singular part of the Gibbs function

$$G = \mathcal{F}(x_1, x_2; \ldots, x_n) \tag{5.4}$$

is an invariant equation under the one-parameter[23] continuous group of transformations $\mathcal{G}$:

$$\mathcal{G}\begin{cases} G' = \lambda G, & \text{(5.5a)} \\ x_i' = \lambda^{a_i}x_i, \quad i = 1, 2, \ldots, n, \quad [a_i = 0,\ i > 2]. & \text{(5.5b)} \end{cases}$$

Equation (5.5) is defined for all positive λ; the a_i are called scaling powers. This statement is equivalent to the scaling hypothesis

$$G(\lambda^{a_1}x_1, \lambda^{a_2}x_2; x_3 \cdots x_n) = \lambda G(x_1, x_2; \cdots x_n). \tag{5.6}$$

For future reference, we will use a superscript s to denote the subgroup generated by the transformations of the independent variables x_i $(i = 1, 2, \ldots, n)$. Thus we may generally define the full group by two equations, where the second denotes the subgroup $\mathcal{G}^s$.

To illustrate the scaling hypothesis when an inactive parameter is present, we consider the example of the antiferromagnet (see Fig. 12). Here we hypothesize that the singular part of the Gibbs potential

$$G = \mathcal{F}_A(H_{st}, x_2, x_3) \tag{5.7}$$

is an invariant equation under the one parameter continuous group of transformations $\mathcal{G}_A$:

$$\mathcal{G}_A\begin{cases} G' = \lambda G, \\ H_{st}' = \lambda^{a_1}H_{st},\ x_2' = \lambda^{a_2}x_2,\ x_3' = x_3, \end{cases} \tag{5.8}$$

where x_2 is a weak direction, $[T - T_c(H)]$ or $[H - H_c(T)]$, and x_3 parametrizes the position of the critical point on the line of critical points. Equivalently G satisfies a GHF equation[24]

$$G(\lambda^{a_1}H_{st}, \lambda^{a_2}x_2; x_3) = \lambda G(H_{st}, x_2; x_3). \tag{5.9}$$

Here H_{st} denotes the staggered magnetic field.

Scaling functions for ferromagnets and antiferromagnets can be obtained the usual way[21] from

Eqs. (5.1) and (5.9), respectively. For example, by setting $\lambda \equiv 1/|H|^{1/a_H}$ in Eq. (5.1), we obtain[25]

$$G(1, \tau/|H|^{a_\tau/a_H}) = |H|^{-1/a_H} G(H, \tau). \tag{5.10}$$

The function $G(H, \tau)$ can be plotted as a curve in a two-dimensional plane with coordinates specified by $G/|H|^{1/a_H}$ and $\tau/|H|^{a_\tau/a_H}$. We note that both $G/|H|^{1/a_H}$ and $\tau/|H|^{a_\tau/a_H}$ are absolute invariants of the group $\mathcal{G}_F$ defined by Eq. (5.3), i.e.,

$$G_H \equiv \frac{G'}{|H'|^{1/a_H}} = \frac{G}{|H|^{1/a_H}}, \tag{5.11a}$$

$$\tau_H \equiv \frac{\tau'}{|H'|^{a_\tau/a_H}} = \frac{\tau}{|H|^{a_\tau/a_H}}, \tag{5.11b}$$

where the second equalities in (5.11) follow from (5.3).

Similarly, by setting $\lambda \equiv 1/|H_{st}|^{1/a_1}$, Eq. (5.9) may be written

$$G(1, x_2/|H_{st}|^{a_2/a_1}; x_3) = |H_{st}|^{-1/a_1} G(H_{st}, x_2; x_3), \tag{5.12}$$

and $G/|H_{st}|^{1/a_1}$, $x_2/|H_{st}|^{a_2/a_1}$, x_3 are absolute invariants of the group $\mathcal{G}_A$. In addition, the last two quantities are absolute invariants of the subgroup $\mathcal{G}_A^s$.

To derive exponents and scaling laws for the antiferromagnet, the procedures developed in Ref. 21 can be simply applied to Eq. (5.9). At points where the critical line is not parallel to the T axis, it is easily shown that

$$\beta = (1 - a_1)/a_2, \tag{5.13a}$$

$$1/\delta = (1 - a_1)/a_1, \tag{5.13b}$$

$$-\gamma = (1 - 2a_1)/a_2, \tag{5.13c}$$

$$-\alpha = (1 - 2a_2)/a_2, \tag{5.13d}$$

where the order parameter M_{st} tends to zero when the critical line is approached in a weak direction with exponent β,

$$M_{st} \propto |T - T_c(H)|^{\beta}, \tag{5.14a}$$

and with exponent $1/\delta$ when it is approached in a strong direction

$$M_{st} \propto H_{st}^{1/\delta}. \tag{5.14b}$$

The staggered susceptibility $\chi_{st} = \partial M_{st}/\partial H_{st}$ diverges with exponent γ,

$$\chi_{st} \propto |T - T_c(H)|^{-\gamma}, \tag{5.14c}$$

and the specific heat at constant order parameter diverges with exponent α:

$$C_{M_{st}} \propto |T - T_c(H)|^{-\alpha}. \tag{5.14d}$$

The last two exponents γ and α refer to weak directions of approach (in the plane $H_{st} = 0$) to the critical line.[26]

In the same way, exponents for the ordinary magnetization M, and ordinary susceptibility $\chi = \partial M/\partial H$ can be derived. It turns out on using Eq. (5.13d) that

$$M - M_c(H) \propto |T - T_c(H)|^{(1-\alpha)}, \tag{5.15a}$$

$$\chi \propto |T - T_c(H)|^{-\alpha}. \tag{5.15b}$$

From Eqs. (5.13a)–(5.13d) the usual scaling law equalities can be derived by eliminating the scaling powers a_1 and a_2:

$$\alpha + 2\beta + \gamma = 2, \qquad \beta(\delta - 1) = \gamma, \quad \beta(\delta + 1) = 2 - \alpha.$$

These results are also obtainable from two simple group invariant theorems which we shall find particularly useful in making the scaling hypothesis for critical subspaces of higher order.

Theorem 1. Consider a one-parameter continuous group of transformations:

$$\mathcal{G}\begin{cases} x_0' = f(\lambda | x_0), & (5.16a) \\ x_i' = f_i(\lambda | x_1, x_2, \ldots, x_n), \quad i = 1, 2, \ldots n. & (5.16b) \end{cases}$$

There exist n functionally independent absolute invariants of the x_i $(i = 0, 1, \ldots, n)$. This theorem is proved in Appendix A.

For our applications, we shall choose the invariants, denoted by y_i $(i = 0, 1, \ldots, n-1)$, such that, for $i = 0$,

$$\frac{\partial y_0}{\partial x_0} \neq 0, \tag{5.17a}$$

and for $i > 0$,

$$(y_1, y_2, \ldots, y_{n-1}) \tag{5.17b}$$

are the $n-1$ functionally independent absolute invariants of the subgroup $\mathcal{G}^s$.

For the simple ferromagnet, $G/|H|^{1/a_H}$ is an absolute invariant under $\mathcal{G}_F$ [see Eq. (5.3)] and $\tau/|H|^{a_\tau/a_H}$ is the functionally independent absolute invariant of (H, τ) under the transformation $\mathcal{G}_F^s$. For the antiferromagnet, $G/|H_{st}|^{1/a_1}$ is an absolute invariant under $\mathcal{G}_A$, and $(x_2/|H_{st}|^{a_2/a_1}, x_3)$ are the *two* functionally independent absolute invariants under $\mathcal{G}_A^s$.

Theorem 2. If

$$x_0 = X_0(x_1, x_2, \ldots, x_n) \tag{5.18}$$

is an invariant equation under $\mathcal{G}$ defined by (5.16) (i.e., if X_0 is a GHF), then it can be expressed as

$$y_0 = Y_0(y_1, y_2, \ldots, y_{n-1}), \tag{5.19}$$

where the y_i $(i = 0, 1, \ldots, n-1)$ form a set of functionally independent absolute invariants of $\mathcal{G}$ given by (5.16), and satisfying (5.17).

The proof of this theorem is given in Appendix B. Equations (5.10) and (5.12) are simple applications of these theorems. The usefulness of theorems 1 and 2 will be apparent in Sec. VI.

VI. SCALING HYPOTHESIS FOR TRICRITICAL POINTS

Before making the scaling hypothesis and examining its consequences for a critical space of arbitrary order $\mathfrak{o}$, we will make it for the special case of a ${}^3R_0$ (tricritical point) for which there are three fields available ($n=3$). This will clarify both notation and concepts, and make passage to the general case more painless.

As was shown in Sec. IV, it is possible at a critical point to select strong and weak directions (directions of types 1 and 2). These we call x_1 and x_2 as before. In a space of total dimension three, the critical subspaces terminating at a ${}^3R_0$ are all ${}^2R_1$. At a point on a ${}^2R_1$ we may select a direction tangent to the line. Thus as one approaches the ${}^3R_0$ along a given ${}^2R_1$, the directions of types 1, 2, and 3 are uniquely defined (see Fig. 14).

Since three critical lines meet at a ${}^3R_0$, three "rival" coordinate systems exist at the point ${}^3R_0$. A scaling hypothesis cannot be made at the tricritical point unless a unique coordinate system can be defined, and this represents an apparent obstacle.

The solution of this problem is somewhat subtle, and the full details have been given in a previous paper.[7(b)] The basic idea is that a scaling hypothesis at the ${}^3R_0$ determines the general shape of a line of critical points near the ${}^3R_0$; thus a scaling hypothesis made in a coordinate system defined by one line will restrict the shapes of the other two lines meeting it (at the tricritical point).

The coordinate systems defined with reference to the other two lines are consistent in the sense that we could have selected any line first to make the scaling hypothesis and we would have obtained the same final result.

To set up a coordinate system in which to make a scaling hypothesis at the ${}^3R_0$, we choose a point P on one of the critical lines (say L_1) and we set up a triad of directions $x_i(L_1)$. Two of these directions are of types 1 and 2, while the third is tangent to the ${}^2R_1$. The coordinate system at the tricritical point is now defined to be

$$\bar{x}_i \equiv \lim_{P \to {}^3R_0} x_i(P) \tag{6.1}$$

(see Fig. 14). The direction $\bar{x}_3$ is of type 3. The bars are used in order that the present notation be consistent with that of Ref. 7(b).

We now introduce a scaling parameter λ ($\lambda > 0$) and make the scaling hypothesis that the singular part of the Gibbs potential is a GHF, i.e.,

$$G(\lambda^{\bar{a}_1}\bar{x}_1, \lambda^{\bar{a}_2}\bar{x}_2, \lambda^{\bar{a}_3}\bar{x}_3) = \lambda G(\bar{x}_1, \bar{x}_2, \bar{x}_3), \tag{6.2}$$

where $(\bar{a}_1, \bar{a}_2, \bar{a}_3)$ are the "tricritical scaling powers". Equation (6.2) is equivalent to the statement that $G = \mathfrak{F}(\bar{x}_1, \bar{x}_2, \bar{x}_3)$ is an invariant equation under the one-parameter continuous group of transformations

$$\mathcal{G}_3 \begin{cases} G' \equiv \lambda G, & \text{(6.3a)} \\ \bar{x}_i' \equiv \lambda^{\bar{a}_i}\bar{x}_i, \quad i = 1, 2, 3. & \text{(6.3b)} \end{cases}$$

According to theorem 1 of Sec. V, the hypothesized invariance property of (6.1) under $\mathcal{G}_3$ implies that there exists a basis set of functionally independent absolute invariants of $\mathcal{G}_3$. We adopt a canonical form for the invariants y_i by scaling $\bar{x}_i$ with respect to the tangent variable—here $\bar{x}_3$—as follows:

$$y_0 \equiv \frac{\bar{x}_0}{\bar{x}_3^{1/\bar{a}_3}}, \quad y_1 \equiv \frac{\bar{x}_1}{\bar{x}_3^{\bar{a}_1/\bar{a}_3}}, \quad y_2 \equiv \frac{\bar{x}_2}{\bar{x}_3^{\bar{a}_2/\bar{a}_3}}, \tag{6.4}$$

with $\bar{x}_0 \equiv G$. Thus, theorem 2 of Sec. V states that $G(\bar{x}_1, \bar{x}_2, \bar{x}_3)$ may be expressed as[27]

$$y_0 = F_2(y_1, y_2). \tag{6.5}$$

Since the variables y_1 and y_2 forms a basis set of functionally independent absolute invariants of the scaling field variables $\bar{x}_1$, $\bar{x}_2$, and $\bar{x}_3$ of the group of transformations $\mathcal{G}_3^s$, any point (k_1, k_2) in the two-dimensional space (y_1, y_2) gives rise to an invariant curve of points in the three-dimensional space $(\bar{x}_1, \bar{x}_2, \bar{x}_3)$. That is, the point given by

$$y_i = k_i, \quad i = 1, 2 \tag{6.6}$$

corresponds to a line in the x_i space that may be conveniently parametrized by

$$(\bar{x}_1, \bar{x}_2, \bar{x}_3) = (k_1\lambda^{\bar{a}_1}, k_2\lambda^{\bar{a}_2}, \lambda^{\bar{a}_3}), \tag{6.7}$$

where λ is an arbitrary parameter (see Fig. 15). In particular the lines of critical points L_j converging on the tricritical point can be expressed in the form of Eq. (6.7), since according to the scaling hypothesis (6.2) they must be invariant under the group of symmetries $\mathcal{G}_3$ of (6.3).

Previously[7(b)] we have derived Eq. (6.7) directly from Eq. (6.2) and demonstrated that if the scaling powers $\bar{a}_i$ are all different, the curves parametrized by Eq. (6.7) end up parallel to the axis $\bar{x}_i$ corresponding to the minimum $\bar{a}_i$ (unless $k_i = 0$). Although the direction of type 3 defined for one line is not necessarily parallel to the direction of type 3 defined for another line, it will at least be parallel to *some* member of the triad defined for that other line. Thus all choices of scaling directions will be mutually consistent![7(b),28]

Along a critical line ${}^2R_1$, the conventional scaling hypothesis is normally stated in terms of a GHF equation of the form

$$G(\mu^{a_1}x_1, \mu^{a_2}x_2; x_3) = \mu G(x_1, x_2; x_3), \tag{6.8}$$

where x_3 is a parameter and does not scale. Near the ${}^3R_0$, however, the shape of the critical line is determined by Eq. (6.7). A ${}^2R_1$ near the ${}^3R_0$ maps into a point (k_1, k_2) in the $y_1 - y_2$ plane given by Eq. (6.6). Furthermore, the value of $y_0 \equiv \bar{x}_0/\bar{x}_3^{1/\bar{a}_3}$

$= G/\bar{x}_3^{1/\bar{a}_3}$ changes only if y_1 and/or y_2 changes. It is therefore more proper to make a precise scaling hypothesis about the critical line ${}^2R_1$ near the ${}^3R_0$ making use of the variables (y_1, y_2).

If we adopt the strong requirement that a point in one phase remains in that phase under the scale transformation $\mathcal{G}_3$, the CXS surfaces become lines in the y_1-y_2 plane. Hence, it is possible to choose the principal directions of scaling for the ${}^2R_{n-2}$ as linear combinations of the variables y_1, y_2.

Because the scaled variables must be zero at the critical line we consider the variables

$$\hat{y}_1 \equiv y_1 - k_1 , \tag{6.9a}$$

$$\hat{y}_2 \equiv y_2 - k_2 . \tag{6.9b}$$

For the line L_1 of Fig. 15, $k_1 = 0$, the coordinate y_1, is everywhere strong and $(y_2 + k)$ is weak. For L_2 and L_3, the weak direction is parallel to the CXS mapped in the $y_1 - y_2$ plane, and both $\hat{y}_1$, $\hat{y}_2$ are strong directions unless the wings end up parallel to one axis.

We therefore define linear combinations of the variables $(y_i - k_i)$, which give the weak and strong directions (they are of necessity also absolute invariants of the group $\mathcal{G}_3$):

$$\tilde{y}_i \equiv \sum_{j=1}^{2} \tilde{R}_{ij}(y_j - k_j), \tag{6.10a}$$

where $\tilde{R}_{ij}$ is a "rotation matrix". Defining

$$\tilde{y}_0 \equiv y_0 , \tag{6.10b}$$

we hypothesize that along a ${}^2R_1$ near the ${}^3R_0$, $\tilde{y}_0$ is a GHF of $(\tilde{y}_1, \tilde{y}_2)$,

$$\tilde{y}_0(\mu^{a_1}\tilde{y}_1, \mu^{a_2}\tilde{y}_2) = \mu\tilde{y}_0(\tilde{y}_1, \tilde{y}_2), \tag{6.11}$$

i.e., $\tilde{y}_0 = \mathcal{F}_2(\tilde{y}_1, \tilde{y}_2)$ is an invariant equation under a group $\mathcal{G}_2$ defined by

$$\mathcal{G}_2 \begin{cases} \tilde{y}_0' = \mu\tilde{y}_0 , & (6.12a) \\ \tilde{y}_i' = \mu^{a_i}\tilde{y}_i , \quad i = 1, 2 . & (6.12b) \end{cases}$$

In general, the group $\mathcal{G}_2$ will be different (having different a_i) for *each* critical line at the tricritical point, and will only be valid within a certain region close to the critical line. The different groups $\mathcal{G}_2$ for the different lines L_i do not have regions of overlap and there is therefore no conflict.

We can now form absolute invariants of $\mathcal{G}_2$. Scaling with respect to the weak direction we obtain

$$z_0 \equiv \frac{\tilde{y}_0}{\tilde{y}_2^{1/a_2}} , \quad z_1 \equiv \frac{\tilde{y}_1}{\tilde{y}_2^{a_1/a_2}} . \tag{6.13}$$

Theorem 2 of Sec. V states that under the hypothesis (6.11), $\tilde{y}_0(\tilde{y}_1, \tilde{y}_2)$ may be expressed as[27]

$$z_0 = \mathcal{F}_1(z_1) . \tag{6.14}$$

The simplest example of this is for the line L_1 of Fig. 15. Here the variables of scaling are

$$\hat{y}_1 = \bar{x}_1 / \bar{x}_3^{\bar{a}_1/\bar{a}_3} , \tag{6.15a}$$

$$\hat{y}_2 = (\bar{x}_2 / \bar{x}_3^{\bar{a}_2/\bar{a}_3} + k) , \tag{6.15b}$$

where k is defined in Fig. 15. Rotation is not necessary and $\tilde{R}_{ij} \equiv \delta_{ij}$. Hence on using (6.13) and (6.15), Eq. (6.14) can be written in the "double-power law" form[27]

$$\frac{G}{\bar{x}_3^{1/\bar{a}_3}(\bar{x}_2/\bar{x}_3^{\bar{a}_2/\bar{a}_3} + k)^{1/a_2}}$$

$$= \mathcal{F}_1\left[\frac{\bar{x}_1}{\bar{x}_3^{\bar{a}_1/\bar{a}_3}(\bar{x}_2/\bar{x}_3^{\bar{a}_2/\bar{a}_3} + k)^{a_1/a_2}}\right]. \tag{6.16}$$

For a simple system with $n = 2$, scaling functions predict data collapsing for functions of two variables from a surface onto a line. For $n = 3$ and functions of three variables, data collapse from a volume onto a surface. However, the double-power scaling function of Eq. (6.16) predicts that data will collapse from a volume onto a line. Clearly this happens only within the region of validity of both groups of transformations $\mathcal{G}_2$ and $\mathcal{G}_3$.

The region of influence of $\mathcal{G}_2$ in the neighborhood of the tricritical point ${}^3R_0$ should also be controlled by the group $\mathcal{G}_3$. This means that the region of influence of $\mathcal{G}_2$ should be bounded by a surface which scales toward the ${}^3R_0$. In Fig. 15, where a line which scales is represented by a point, a surface which scales will be represented by a line. We therefore plot the surfaces bounding the region of influence of the group $\mathcal{G}_2$ (of transformations about a ${}^2R_1$, L_i) as a line surrounding the point in the y_1-y_2 plane, representing the particular line L_i.

In terms of the variables y_1, y_2 such a line will be represented by the equation

$$f(y_1, y_2) = 0 \tag{6.17a}$$

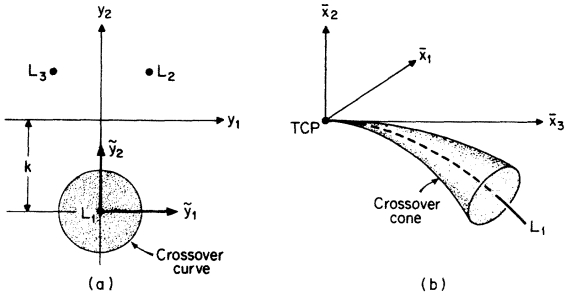

FIG. 15. (a) Plot of the invariants (y_1, y_2) for the group $\mathcal{G}_3$ of transformations about the tricritical point. The strong and weak directions for the line L_1 are y_1 and y_2. The circle around L_1 is a possible shape for the crossover region. (b) The principal points of interest of Fig. 15(a) in the full space $(\bar{x}_1, \bar{x}_2, \bar{x}_3)$. The point labeled L_1 has become a line and the circle surrounding it has become a cone.

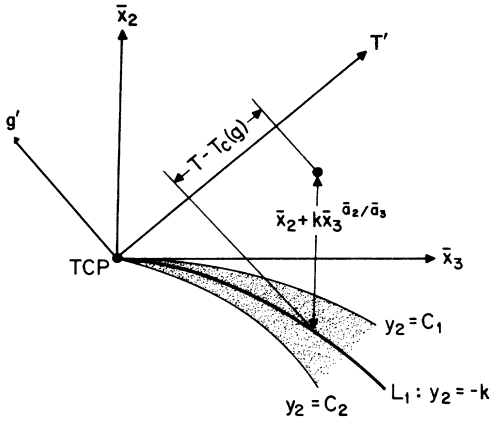

FIG. 16. Figure 15(b) sliced in the $\bar{x}_2$, $\bar{x}_3$ plane. The cone has become the two lines labeled $y_2=C_1$, C_2 [see Fig. 15(a)]. These are generally referred to as crossover lines: $(T',g')=(T-T_t,g-g_t)$.

or

$$f(\bar{x}_1/|\bar{x}_3|^{\bar{a}_1/\bar{a}_3},\ \bar{x}_2/|\bar{x}_3|^{\bar{a}_2/\bar{a}_3})=0\,. \tag{6.17b}$$

The area bounded by this curve (6.17) maps into a conical volume surrounding the critical line L_1 (Fig. 15). Scaling will not tell us the actual shape of the curve in the y_1-y_2 plane but it does limit the shape in the $(\bar{x}_1,\bar{x}_2,\bar{x}_3)$ space, since all points in the y_1-y_2 plane give rise to curves approaching the tricritical point along a particular direction—the axis corresponding to the minimum $\bar{a}_t$.

In the plane $\bar{x}_1=0$, Eq. (6.16) requires[29] that

$$G\propto \bar{x}_3^{1/\bar{a}_3}(\bar{x}_2/\bar{x}_3^{\bar{a}_2/\bar{a}_3}+k)^{1/a_2}\,, \tag{6.18}$$

and the conical surface of Eq. (6.17) becomes the two "crossover lines"

$$\bar{x}_2=C_{1,2}\bar{x}_3^{\bar{a}_2/\bar{a}_3}\,, \tag{6.19}$$

as shown in Fig. 16. The crossover exponent φ,[7(a)] given by

$$\varphi\equiv\bar{a}_3/\bar{a}_2\,, \tag{6.20}$$

determines the shape of the crossover lines, and it can be determined directly from the shape of the line L_1 ($^2R_1$).

The lines are called crossover lines, because the behavior of a particular function crosses over from an exponent characteristic of the $^3R_0$ far away from the line, to an exponent characteristic of the $^2R_1$ at points close to the $^2R_1$. It is important to realize that the group $\mathcal{G}_3$ does not cease to be valid, and the crossover does not refer to changing from one group to another. The group $\mathcal{G}_3$ is everywhere valid, and the crossover merely marks the limits of validity of $\mathcal{G}_2$. This principle will be extended in Paper II and the groups $\mathcal{G}_j$ will control crossovers (or boundaries for the regions of validity) of $\mathcal{G}_i$ where $j>i$.

Finally, a few remarks should be made about the exponents and the directions of approach to the tricritical point. Equation (6.18) shows that if $\bar{x}_2/|\bar{x}_3|^{\bar{a}_2/\bar{a}_3}$ is a constant the exponent for G is $1/\bar{a}_3$. For a function f with a tricritical-point (TCP) scaling power $\bar{a}_f$, and a critical-line scaling power a_f, the equation analogous to Eq. (6.18) predicts exponents $\bar{a}_f/\bar{a}_3$ and a_f/a_2. For example, for the staggered susceptibility $\chi_{st}\equiv\partial^2G/\partial H_{st}^2$, from (6.16),

$$\chi_{st}\propto\bar{x}_3^{(1-2\bar{a}_1)/\bar{a}_3}(\bar{x}_2/\bar{x}_3^{\bar{a}_2/\bar{a}_3}+k)^{(1-2a_1)/a_2}\,, \tag{6.21}$$

and $\bar{a}_f=1-2\bar{a}_1$ and $a_f=1-2a_1$ for this case. Thus for all the exponents considered below the numerators can be appropriately be replaced by $\bar{a}_f$ or a_f.

If the $^3R_0$ is approaches along a direction not asymptotically parallel to the $\bar{x}_3$ axis (i.e., outside the crossover lines), G scales with a power $1/\bar{a}_2$.

If the $^2R_1$ is approached along a line of constant $\bar{x}_3$, in the plane $\bar{x}_1=0$ Eq. (6.18) shows that G has an exponent $1/a_2$. This is expected, of course, since G has an exponent $1/a_2$ for any point (i.e., fixed x_3) on the line $^2R_1$ even when the point is far away from the $^3R_0$ [see Eq. (6.8)].

In Sec. V, exponents were demonstrated in terms of the scaling powers a_t [Eqs. (5.13)] and the same can be done here for the $^2R_1$ (exponents in terms of a_t) and the $^3R_0$ (exponents in terms of the $\bar{a}_t$) separately. The only new exponents, which will be derived, are exponents for the directions of approach to the $^3R_0$ along $y_2=$ constant and these give exponents of the form

$$f\sim|x_3|^{\bar{a}_f/\bar{a}_3}\,. \tag{6.22}$$

These can be related to exponents of approach along directions of type 2 by relations of the form

$$\bar{a}_f/\bar{a}_3=(\bar{a}_f/\bar{a}_2)/\varphi. \tag{6.23}$$

These are new predictions of scaling specific to tricritical points [the others are analogous to Eq. (5.13)].[7(c)]

Finally, we emphasize the importance of expressing the scaling relations in terms of invariants. For example, Eq. (6.21) may be written in the alternative "mixed-exponent form"

$$\chi_{st}\propto C(\bar{x}_2+k\bar{x}_3^{1/\varphi})^{-\gamma}\,, \tag{6.24}$$

where

$$C\propto\bar{x}_3^{(\gamma-\bar{\gamma})/\varphi}\,, \tag{6.25}$$

with

$$-\gamma=\frac{1-2a_1}{a_2}\,,\qquad -\bar{\gamma}=\frac{1-2\bar{a}_1}{\bar{a}_2}\,. \tag{6.26}$$

Expressions (6.24) and (6.25) appear more complicated than they actually are. The exponents are actually not mixed when expressed in the invariant from as shown in Eq. (6.21).

ACKNOWLEDGMENTS

We wish to thank F. Harbus, R. B. Griffiths, J. C. Wheeler, and E. K. Riedel for stimulating discussions.

APPENDIX A: PROOF OF THEOREM 1

Theorem 1. Consider a one-parameter continuous group of transformations

$$\mathcal{G}:\ x_i' = f_i(\lambda \mid x_0, x_1, \ldots, x_n), \tag{A1}$$

where $i = 0, 1, \ldots, n$. There exist n functionally independent absolute invariants of the x_i $(i = 0, 1, \ldots, n)$.

Proof of theorem 1. Consider a function $F(x_0', x_1', \ldots, x_n')$. Assume the derivatives of f_i with respect to λ exist. We expand $F(x_0', x_1', \ldots, x_n')$ in a Maclaurin series

$$F(x_0', x_1', \ldots, x_n') = f + f'(\delta\lambda) + \frac{f''}{2!}(\delta\lambda)^2 + \cdots, \tag{A2}$$

where

$$\begin{aligned} f &= F(x_0, x_1, \ldots, x_n), \\ f' &= \left(\frac{dF}{d\lambda}\right)_{\lambda=\lambda_0} = VF(x_0, x_1, \ldots, x_n), \\ f'' &= \left(\frac{d^2F}{d\lambda^2}\right)_{\lambda=\lambda_0} = V^2F(x_0, x_1, \ldots, x_n), \\ &\vdots \end{aligned} \tag{A3}$$

with λ_0 the value of λ corresponding to the identical transformation and

$$V \equiv \sum_{i=0}^{n} \xi_i \left(\frac{\partial}{\partial x_i}\right), \tag{A4}$$

$$\xi_i \equiv \left(\frac{\partial f_i}{\partial \lambda}\right). \tag{A5}$$

If, therefore, $F(x_0, x_1, \ldots, x_n)$ is an absolute invariant of the group $\mathcal{G}$, then

$$F(x_0', x_1', \ldots, x_n') = F(x_0, x_1, \ldots, x_n). \tag{A6}$$

The necessary and sufficient condition for $F = \text{const}$ is that

$$VF = \sum_{i=0}^{n} \xi_i \left(\frac{\partial F}{\partial x_i}\right) = 0. \tag{A7}$$

Thus, F is a solution of the partial differential equation (A7) and consequently, $F(x_0, x_1, \ldots, x_n) = \text{const}$ is a solution of the system of the equivalent ordinary differential equations

$$\frac{dx_0}{\xi_0} = \frac{dx_1}{\xi_1} = \cdots = \frac{dx_n}{\xi_n}. \tag{A8}$$

These equations admit n independent solutions (first integrals)[30,31] and theorem 1 is proved.

APPENDIX B: PROOF OF THEOREM 2

Theorem 2. If the equation

$$x_0 = X_0(x_1, x_2, \ldots, x_n) \tag{B1}$$

is invariant under

$$\mathcal{G}\begin{cases} x_0 = f(\lambda \mid x_0), \\ x_i' = f_i(\lambda \mid x_1, x_2, \ldots, x_n), \end{cases} \tag{B2}$$

then it can be expressed as

$$y_0 = Y_0(y_1, y_2, \ldots, y_{n-1}), \tag{B3}$$

where $(y_0, y_1, \ldots, y_{n-1})$ form a set of functionally independent absolute invariants under $\mathcal{G}$, with

$$\frac{\partial y_0}{\partial x_0} \neq 0,$$

and $(y_1, y_2, \ldots, y_{n-1})$, the $n-1$ functionally independent absolute invariants of $\mathcal{G}^s$.

By hypothesis, y_0 is an absolute invariant of $(x_0; x_1, \ldots, x_n)$ of $\mathcal{G}$. Thus, (B3) implies that the invariant equation (B1) may be written

$$y_0(x_0; x_1, x_2, \ldots, x_n) = Y_0(y_1, y_2, \ldots, y_{n-1}). \tag{B4}$$

Since $(y_1, y_2, \ldots, y_{n-1})$ form a basis set of functionally independent absolute invariants of $(x_1, x_2, \ldots, x_n)$ of $\mathcal{G}^s$, (B4) is equivalent to the statement that x_0 is expressible as an implicit function of $(x_1, x_2, \ldots, x_n)$:

$$y_0(x_0; x_1, x_2, \ldots, x_n) = g(x_1, x_2, \ldots, x_n), \tag{B5}$$

where g is an absolute invariant of $(x_1, x_2, \ldots, x_n)$ under $\mathcal{G}^s$.

Before we launch into the proof of the theorem, we give a proof of the following lemma.[32]

Lemma. A necessary and sufficient condition for x_0, implicitly defined by (B5), as a function of $(x_1, x_2, \ldots, x_n)$, to be the same function as x_0' of $(x_1', x_2', \ldots, x_n')$ implicitly defined by

$$y_0(x_0', x_1', x_2', \ldots, x_n') = g'(x_1', x_2', \ldots, x_n') \tag{B6}$$

is that g is an absolute invariant of $(x_1, x_2, \ldots, x_n)$ under $\mathcal{G}^s$.

Proof of lemma. Since y_0 is an absolute invariant of $\mathcal{G}$, we have

$$y_0(x_0; x_1, x_2, \ldots, x_n) = y_0(x_0'; x_1', x_2', \ldots, x_n'). \tag{B7}$$

Since we require $x_0(x_1, x_2, \ldots, x_n)$ to be exactly the same function as $x_0'(x_1', x_2', \ldots, x_n')$, (B5)–(B7) require that

$$\begin{aligned} g(x_1, x_2, \ldots, x_n) &= g'(x_1', x_2', \ldots, x_n') \\ &= g(x_1', x_2', \ldots, x_n'). \end{aligned} \tag{B8}$$

This is the necessity proof.

We now demonstrate (B8) is sufficient to ensure (B5) and (B6) admit an invariant solution such that

$x_0(x_1, x_2, \ldots, x_n)$ is exactly the same function as $x_0'(x_1', x_2', \ldots, x_n')$. Inverting (B5) and (B6), we obtain

$$x_0(x_1, x_2, \ldots, x_n) = h(g; x_1, x_2, \ldots, x_n),$$
$$x_0'(x_1', x_2', \ldots, x_n') = h'(g'; x_1, x_2, \ldots, x_n), \tag{B9}$$

in some neighborhood of the $(x_1, x_2, \ldots, x_n)$ and $(x_1', x_2', \ldots, x_n')$ spaces, respectively. It is obvious that $h(g; x_1, x_2, \ldots, x_n)$ is exactly the same function as $h'(g_1'; x_1', x_2', \ldots, x_n')$. But, by hypothesis, $g(x_1, x_2, \ldots, x_n)$ is exactly the same function as $g'(x_1', x_2', \ldots, x_n')$. Therefore, $x_0(x_1, x_2, \ldots, x_n)$ is exactly the same function as $x_0'(x_1', x_2', \ldots x_n')$.

Proof of theorem 2. Using the lemma and the fact that $g(x_1, x_2, \ldots, x_n)$ in (B5) is an absolute invariant of $(x_1, x_2, \ldots, x_n)$ under $\mathcal{G}^s$, we immediately verify the statement of theorem 2.

APPENDIX C: PROOF OF THEOREM 3

Theorem 3. Consider a one-parameter continuous group of transformations $\mathcal{G}$:

$$\mathcal{G}\begin{cases} x_0' = \lambda x_0, \\ x_i' = f_i(\lambda) x_i, \quad i = 1, 2, \ldots, n. \end{cases} \tag{C1}$$

If

$$x_0 = F(x_1, x_2, \ldots, x_n) \tag{C2}$$

is an invariant equation under $\mathcal{G}$, the most general form for $f_i(\lambda)$ is λ^{a_i}, where a_i are constants.

Proof of theorem 3. We transform (C2) by means of (C1) for two successive values of $\lambda = \lambda_1$, λ_2,

$$\lambda_1\lambda_2 x_0 = F[f_1(\lambda_1)f_1(\lambda_2)x_1, f_2(\lambda_1)f_2(\lambda_2)x_2, \ldots, f_n(\lambda_1)f_n(\lambda_2)x_n], \tag{C3}$$

and again for the value of $\lambda = \lambda_1\lambda_2$,

$$\lambda_1\lambda_2 x_0 = F[f_1(\lambda_1\lambda_2)x_1, f_2(\lambda_1\lambda_2)x_2, \ldots, f_n(\lambda_1\lambda_2)x_n]. \tag{C4}$$

These results are to hold for all values of x_i. Setting $x_2 = x_3 = \cdots = x_n = 0$, we have from (C3) and (C4)

$$F[f_1(\lambda_1)f_1(\lambda_2)x_1, 0, \ldots, 0] = F[f_1(\lambda_1\lambda_2)x_1, 0, \ldots, 0]. \tag{C5}$$

Therefore,

$$f_1(\lambda_1)f_1(\lambda_2) = f_1(\lambda_1\lambda_2). \tag{C6}$$

The solution[33] of the functional equation for $f_1(\lambda)$ for $\lambda > 0$ is

$$f_1(\lambda) = \lambda^{a_1}, \tag{C7}$$

where a_1 is a constant. This process may be repeated for each $f_1(\lambda)$, $i = 1, 2, \ldots, n$. Thus, theorem 3 is proved.

---

*Work forms a part of a Ph.D. thesis to be submitted to the Physics Department of MIT by A. Hankey. Preliminary reports of aspects of this work appear in T. S. Chang, A. Hankey, and H. E. Stanley, AIP Conf. Proc. **10**, 880 (1973).

†Supported by NSF Grant No. GU-1590 and NASA Grant No. NGL 34-002-084. Permanent address: Riddick Laboratories, North Carolina State University, Raleigh, N.C. 27607.

‡Supported by a Research Assistantship from the Laboratory for Nuclear Science, MIT Lindemann Fellow. Present address: SLAC, Stanford, Calif.

§Supported by NSF, ONR. and AFOSR

[1]A. Hankey, T. S. Chang, and H. E. Stanley, Phys. Rev. B (to be published), hereafter referred to as II. See also, F. Harbus, A. Hankey, H. E. Stanley, and T. S. Chang, Phys. Rev. B (to be published).

[2](a) B. Widom, J. Chem. Phys. **43**, 3892 (1965); (b) C. Domb and D. L. Hunter, Proc. Phys. Soc. Lond. **86**, 1147 (1965); (c) L. P. Kadanoff, Physics (N.Y.) **2**, 263 (1966); (d) R. B. Griffiths, Phys. Rev. **158**, 176 (1967).

[3]E. K. Riedel and F. Wegner, Z. Phys. **225**, 195 (1969).

[4]E. K. Riedel and F. Wegner, Phys. Rev. Lett. **24**, 730 (1970).

[5]R. B. Griffiths and J. C. Wheeler, Phys. Rev. A **2**, 1047 (1970).

[6]R. B. Griffiths, Phys. Rev. Lett. **24**, 715 (1970).

[7](a) E. K. Riedel, Phys. Rev. Lett. **28**, 675 (1972); (b) A. Hankey, H. E. Stanley, and T. S. Chang, Phys. Rev. Lett. **29**, 278 (1972). (c) See also, R. B. Griffiths, Phys. Rev. B **7**, 545 (1973).

[8]J. F. Nagle, Phys. Rev. A **2**, 2124 (1970); J. F. Nagle and J. C. Bonner, J. Chem. Phys. **54**, 729 (1971); J. C. Bonner and J. F. Nagle, J. Appl. Phys. **42**, 1280 (1971).

[9]We will use the word "spaces" to mean subspaces of the total space of field or fieldlike variables. Fieldlike refers to variables which occur as parameters in the Hamiltonian and which are *not* discontinuous across coexistence surfaces.

[10](a) E. H. Graf, D. M. Lee, and J. D. Reppy, Phys. Rev. Lett. **19**, 417 (1967). These authors only treat the tricritical point at the lowest pressure. See also, G. Goellner and H. Meyer, Phys. Rev. Lett. **26**, 1543 (1971); and G. Goellner, Ph.D. thesis (Duke University, 1972) (unpublished). (b) W. B. Yelon (private communication); see also, C. W. Garland and B. B. Weiner, Phys. Rev. B **3**, 1634 (1971).

[11]Parameters in a Hamiltonian which can be varied have similar properties to field variables with respect to the geometry of the surfaces. These are used in Sec. III.

[12](a) F. J. Wegner, Phys. Rev. B **5**, 4529 (1972); (b) Phys. Rev. B **6**, 1891 (1972); (c) E. K. Riedel and F. J. Wegner, Phys. Rev. Lett. **29**, 349 (1972).

[13]I. S. Jacobs and P. E. Lawrence, Phys. Rev. **164**, 866 (1967); V. A. Schmidt and S. A. Friedberg, Phys. Rev. B **1**, 2250 (1970); B. E. Keen, D. P. Landau, B. Schneider, and W. P. Wolf, J. Appl. Phys. **37**, 1120 (1966); W. B. Yelon and R. J. Birgeneau, Phys. Rev. B **5**, 2615 (1972); F. Harbus and H. E. Stanley, Phys. Rev. Lett. **29**, 58 (1972); Phys. Rev. B (to be published).

[14]For an elementary account of anisotropic antiferromagnets, including a brief discussion of the spin-flop transition, see, e.g., D. H. Martin, *Magnetism in Solids* (MIT Press, Cambridge, Mass., 1967), pp. 261–263. The implications of scaling here are touched on in A. Hankey, Ph.D. thesis (MIT, 1973)(unpublished).

[15]W. K. Theuman and J. S. Hoye, J. Chem. Phys. **55**, 4159 (1971); see also P. C. Hemmer and G. Stell, Phys. Rev. Lett. **24**, 1284 (1970); and G. Stell and P. C. Hemmer, J. Chem. Phys. **56**, 2474 (1972); A. Hankey, Ref. 14.

[16]A more complete account of these models will be given else-

where; a preliminary account appears in A. Hankey, T. S. Chang, and H. E. Stanley, AIP Conf. Proc. 10, 899 (1973).

[17]This point occurs when $2mH = 2J_{SR}$, where $2m = 1$, in the remainder of this work and J_{SR} is the nearest-neighbor exchange energy [cf. Eq. (3.1)].

[18]The inclusion of a competing long-range interaction makes it possible to define a fourth variable, which is fieldlike, although it is strictly not a field. This variable is the ratio of interaction strengths in the Hamiltonians. In the figures, it is denoted by $\tilde{\mathcal{R}} \equiv J_{SR}/J_{LR}$. This variable is "fieldlike" because the CXS and CRS in the space including $\tilde{\mathcal{R}}$ have the same properties as in spaces of fields.

[19]An exact analysis of an Ising model with several staggered fields requires consideration of a regularly repeating block of spins. The length of the block will be equal to the lowest common multiple of the wavelengths of the various staggered fields. If staggered fields of wavelengths 2 and 3 had been chosen, there would be six spins in a block, but with wavelengths 2 and 4, there are only four spins per block. The analysis for a block of n spins proceeds by multiplying together n transfer matrices and so H_2 and H_4 give the smallest number of matrices to multiply.

[20]Our ideas of using the invariant theorems of continous groups of transformations for multicomponent scaling were first presented at the MIT Summer School on Critical Phenomena in 1971 (unpublished). Recently, important advances have been made by Wilson, Fisher, Wegner, Riedel and others in generating the scaling exponents using the linearized renormalization group equations. It was shown that the scaling fields may be deduced from the relevant operator densities. The number of references to work utilizing the renormalization group now exceeds 100, and the reader is urged to consult K. G. Wilson, Phys. Reports (to be published) or *Cooperative Phenomena Near Phase Transitions: A Bibliography with Selected Readings*, edited by H. E. Stanley (MIT Press, Cambridge, Mass., 1973).

[21]This form of the scaling hypothesis has been treated in detail by A. Hankey and H. E. Stanley [Phys. Rev. B **6**, 3515 (1972)]. It is a more complete discussion of the statements of the hypothesis previously used by Riedel and Wegner (Refs. 3 and 4) and also by Kadanoff (Ref. 2c). For a complete set of references, see *Cooperative Phenomena near Phase Transitions: A Bibliography with Selected Readings,* edited by H. E. Stanley (MIT Press, Cambridge, Mass., 1973).

[22]The elements of the group are parametrized by the single parameter λ. Thus the group is a one-parameter group.

[23]A more-general linear transformation will be $x_i = f_i(\lambda)x_i$. Because of the associativity property of groups, it can be shown that $f_i(\lambda) = \lambda^{a_i}$ [Appendix C]. If some of the x_i do not scale and serve only as "inactive parameters" in Eq. (5.6), the corresponding scaling powers are equal to zero.

[24]We could, of course, replace H_{st} by x_1 in Eq. (5.9), but we emphasize that (cf. Fig. 12) the only thermodynamic field axis which is a strong direction is H_{st}. Thus while the direction $H_{st} + \epsilon(H - H_c)$ or $H_{st} + \epsilon(T - T_c)$ are both strong and $\partial/\partial H_{st}$ is the same as $\partial/\partial x_1$, $\partial/\partial T$, and ∂/∂H are only equivalent to differentiating with respect to x_2.

[25]Here we will formulate the scaling hypothesis only for the Gibbs function, because the scaling equation analogous to (5.1) for other functions can be obtained by appropriate differentation with respect to its independent variables. Scaling functions for physcially more interesting functions like M and χ can then be obtained by the same method used here for G.

[26]Equations (5.14) can all be written in terms of $|H - H_c(T)|$ except at the Néel point, where the line of critical points is parallel to the H axis.

[27]Occasionally, it turns out to be appropriate to scale with respect to a variable which is not tangent—see, e.g., Paper II. This is also true when all the ${}^2R_1$ do not end up parallel and the tangent variable for one line is *not* the tangent variable for another line. We emphasize that scaled equations may change their values or functional forms when the scaling variables change signs.

[28]"Mutually consistent" means that if one chooses two different sets of axes for scaling, one set $(\bar{x}_1, \bar{x}_2, \bar{x}_3)$ with reference to a line L and the second $(\bar{x}_1', \bar{x}_2', \bar{x}_3')$ with repsect to L', then the second set is none other than a permutation of the first set.

[29]Our expression differs from that given in Ref. 7 [Eq. (8)], where the constant k is not present. The constant k is needed to ensure the divergence property of χ_{st} (and other second derivatives of G) along the critical line.

[30]L. P. Eisenhart, *Continuous Groups of Transformations* (Princeton U. P., Princeton, N.J., 1933).

[31]L. S. Pontryagin, *Ordinary Differential Equations* (Addison-Wesley, Reading, Mass., 1962).

[32]A. J. A. Morgan, Q. J. Math. **2**, 250 (1952).

[33]J. Aczèl, *Lectures on Functional Equations and their Applications* (Academic, New York, 1966).